FACILITY SITING STUDY OF LNG-FSRU SYSTEM BASED ON QUANTITATIVE MULTI-HIERARCHY FRAMEWORK MADA

A Thesis

by

CHENXI JI

Submitted to the Office of Graduate and Professional Studies of
Texas A&M University
in partial fulfillment of the requirements for the degree of

MASTER OF SCIENCE

Chair of Committee,	M. Sam Mannan
Committee Members,	Mahmoud M. El-Halwagi
	Li Zeng
Head of Department,	M. Nazmul Karim

December 2017

Major Subject: Safety Engineering

ABSTRACT

This research proposed to establish a quantitative assessment framework for a site selection study of liquefied natural gas (LNG) receiving terminal by considering both chemical process safety and marine transportation safety.

The offshore LNG terminal, referred as LNG floating storage unit (FSU) or floating storage and re-gasification unit (FSRU), performs well on both building and operation processes. The LNG FSRU system is a cost-effective and time efficient solution for LNG transferring in the offshore area, and it brings minimal impacts to the surrounding environment as well. This paper proposed an evaluation framework for LNG FSRU system site selection. The evaluation framework was adopted to process a comparison study between two possible locations for LNG offshore FSU/FSRU. This research divided the whole process into three, beginning with the LNG Carrier navigating in the inbound channel, through the berthing operation and ending with the completion of LNG transferring operation. The preferred location is determined by simultaneously evaluating navigation safety, berthing safety and LNG transferring safety objectives based on the quantitative multi-hierarchy framework multi-attribute decision analysis (QMFMADA) method. The maritime safety analysis, including navigational process and berthing process, was simulated by LNG ship simulator DMU V-Dragon 3000A and analyzed by statistical software such as R and JMP. The chemical process safety simulation was employed to LNG transferring events such as connection hose

rupture, flange failure by the consequence simulation tool Safeti. Two scenarios, *i.e.*, worst case scenario and maximum credible scenario, were taken into consideration by inputting different data of evaluating parameters. The QMFMADA method transformed the evaluation criteria to one comparable unit, risk utility value, to evaluate the different alternatives. Based on the final value of the simulation, the preferred location can be determined and the mitigation measures were presented accordingly.

DEDICATION

This thesis is dedicated to

my parents, Xiumin Ji and Qingxiu Du

and

my loved Chaoyao Yu

ACKNOWLEDGEMENTS

I would like to express my deepest appreciation to my advisor, Dr. M. Sam Mannan for his excellent guidance, caring, patience, and providing me with a unique platform for doing research with him.

I would also like to thank my committee members, Dr. Mahmoud M. El-Halwagi, and Dr. Li Zeng for their precious comments and suggestions on my research projects and the scientific thinking.

Thanks also go to my friends and colleagues and the department faculty and staff for making my time at Texas A&M University a great experience. Finally, thanks to my fiancée for her encouragement, patience and love.

CONTRIBUTORS AND FUNDING SOURCES

Contributors

This work was supervised by a thesis committee consisting of Professor M. Sam Mannan and Professor Mahmoud M. El-Halwagi of the Department of Chemical Engineering and Professor Li Zeng of the Department of Industrial and Systems Engineering.

All work for the thesis was completed independently by the student.

Funding Sources

There are no outside funding contributions to acknowledge related to the research and compilation of this document.

NOMENCLATURE

AHP	Analytic Hierarchy Process
APF	Average Possibility of Fatality
BLEVE	Boiling Liquid Expanding Vapor Explosion
ESDS	Emergency Shut Down System
FLNG	Floating Liquefied Natural Gas
FSRU	Floating Storage and Re-gasification Unit
LNGC	Liquefied Natural Gas Carrier
MADA	Multi-Attribute Decision Analysis
MCS	Maximum Credible Scenario
PLL	Potential Loss of Life
QMFMADA	Quantitative Multi-Hierarchy Framework MADA
RPT	Rapid Phase Transition
RUV	Risk Utility Value
TDU	Thermal Dose Unit
UDM	Unified Dispersion Model
UKC	Under Keel Clearance
VCE	Vapor Cloud Explosion
WCS	Worst Case Scenario

TABLE OF CONTENTS

LIST OF FIGURES

Page

LIST OF TABLES

Page

CHAPTER I

INTRODUCTION

1.1 Background

Liquefied natural gas (LNG) liquefied via dehydration, de-heavy hydrocarbons, and deacidified. Meanwhile, the volume of LNG is approximately equal to 1/600 of that of natural gas [1]. Therefore, the high storage efficiency, low cost, and economical long-distance transportation are the main advantages of LNG. In addition, LNG can be optimized industrial and civil fuel because of its eco-friendliness and high calorific value.

Currently, LNG Carrier (LNGC) is the most common tool for long-distance transportation between natural gas plants and traditional LNG terminals. Since the technique of floating production, storage, and offloading keeps developing these years, many new loading and discharging modes are put into use in the offshore area. The typical LNG supply chain starts at the gas exploration plants [2]. LNG is liquefied and stored in the export terminal; through the LNGC, LNG can be transferred to import terminal to store and to carry out re-gasification process before it is sent to downstream customers for civil or industrial utilizations. A floating LNG unit can substitute the traditional export terminal, acting as a liquefaction plant and LNG storage offshore, this is called floating liquefied natural gas (FLNG). On the other side, to take the place of a

traditional import LNG terminal, a technology called LNG floating storage and re-gasification unit (FSRU) was adopted to store the transferred LNG and to convert the LNG to gaseous state to meet the requirements of civil and industry utilization [3].

1.2 LNG FSRU

As shown in Figure 1, the typical LNG supply chain includes gas exploration, export terminal, LNG carrier, import terminal and pipelines. LNG FSRU, which is employed to improve working efficiency of LNG import terminal, integrates the storage function with re-gasification plant, locating in the offshore or near shore areas.

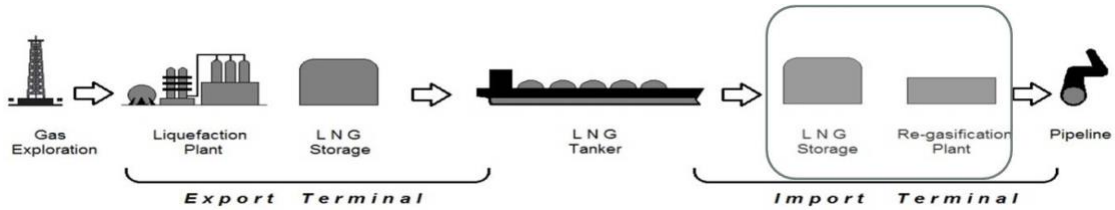

Figure 1. LNG Supply Chain (Adapted from [4])

Compared with traditional LNG receiving terminals, LNG-FSRU performs better on many aspects. Building time saving: an LNG-FSRU is typically commissioned in 2 years, while an onshore LNG terminal usually takes 4-5 years; Flexible to re-location: typical LNG-FSRU systems are reconfigured by LNGCs, and since they still can serve as a transportation tool, when the natural gas market grows, it can be relocated in another area to solve supply and demand problems like the emergent shortage of natural gas;

Cost-effective, the investment of LNG-FSRU is usually 4 to 5 times less than that of land LNG receiving terminal [5].

1.3 Research Objective

This research defines a LNG FSRU system, including the LNG carrier (LNGC) which is to be berthed alongside the FSRU, the FSRU itself and the operation interaction of LNGC and FSRU. It starts from the LNGC entering into the inner harbor area via inbound channel and ends with the completion of LNG transferring. Three events are involved in the research, LNGC navigation, LNGC berthing alongside the LNG FSRU and cargo transferring operation between LNGC and LNG FSRU.

The research objective is to perform an offshore facility, LNG FSRU, siting evaluation by integrating both maritime safety and chemical process safety knowledge. To fulfill it, the safety performance evaluation framework of the LNG FSRU system should be established by risk evaluation methods, and this framework is formulated to make a decision on the location of two alternatives as a case study. To build the safety evaluation framework, one improved multi-attribute decision analysis (MADA) is adopted to assess the different hierarchies layer by layer from bottom to top. Furthermore, the weight vectors and utility values should be determined by calculation. The final decision can be made by analyzing the output of total utility values of the different alternatives accordingly.

The evaluation process starts with the LNGC entering the inner harbor channel, after the LNGC berthing alongside FSRU and ends with the completion of LNG cargo transferring, see Figure 2.

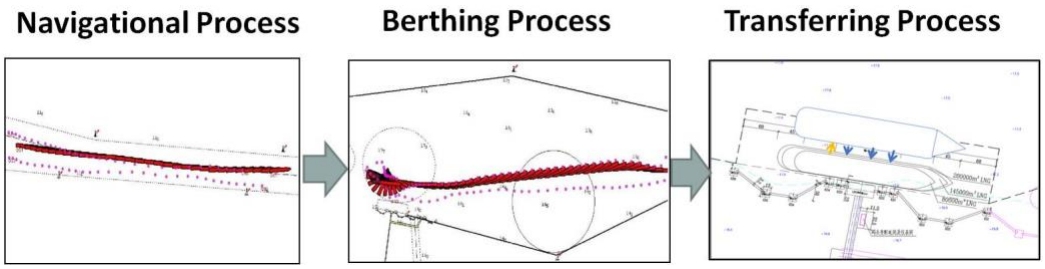

Figure 2. Defined Evaluation Processes

Three processes are comprised in this research:

- Navigational Safety: LNGC Navigating in the inner harbor channel;
- Berthing Safety: LNGC Berthing operation in the turning basin area;
- Operational Safety: LNG offloading process from LNGC to LNG FSRU.

1.4 Research Methodology

The Multi-attribute decision analysis (MADA) was employed to obtain the preferred decision of building one LNG FSRU system. MADA is an optimum decision-making method to get the output of overall utility function, which is constituted by weight vectors multiplied by utility values. Based on the calculated overall utility value

of each alternative, the preferred decision can be made with the maximum expected utility value [6].

Analytic Hierarchy Process (AHP) was firstly proposed by Dr. Saaty in the 1970s to solve decision making problems by evaluating different factors from bottom hierarchy to the highest one [7].

Since the MADA is good at dealing with the decision-making problems among several attributes in one layer, and the AHP outperforms for different layer determination. By putting use of these two theories, this research improved MADA and AHP to a quantitative multi-hierarchy framework MADA (QMFMADA). The core idea of this method to divide the top problem into several processes first, then different processes are evaluated individually by various quantitative tools such as risk simulation software such as Safeti, ship simulator and data analysis software R. Next step is for hazard identification: major hazards are identified under different processes. To quantitatively evaluate different hazards, previous theories and equations may be referred to determine the major attributes which are under the hazard layer. By considering the data availability, the attribute layers can still go down to sub factor layers to quantitatively evaluate the top object directly. Put simply, the framework determination of QMFMADA is a top-to-bottom work, and then the final evaluation is a bottom-to-top progress, see Figure 3.

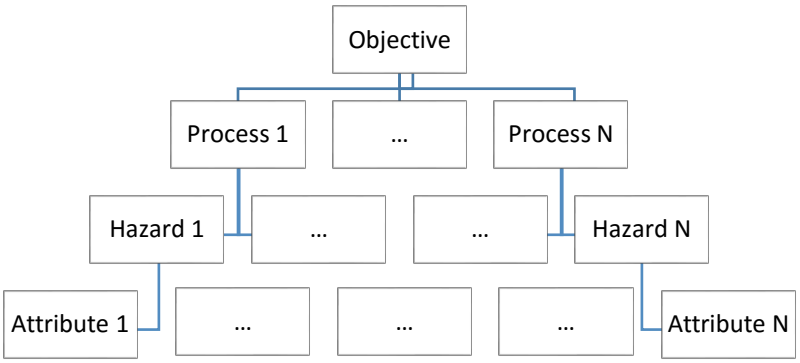

Figure 3. Proposed Evaluation Framework of QMFMADA

CHAPTER II

LITERATURE REVIEW

2.1 Hazard Identification

To establish the framework shown in Figure 3, it is necessary to determine the hazard hierarchy after the process layer has been defined in Figure 2. Generally, hazards are identified by hazard and operability study (HAZOP), Failure mode, effects and criticality analysis (FMECA), and What-if analysis. According to Paltrinieri, 2015, the typical hazards identified for an LNG-FSRU system are: contact with cryogenic liquid, pool fire, flash fire, rapid phase transition (RPT), stranding, contacting with other objects in the vicinity, and leaking during cargo transferring [8].

During 1964 to 2015, there are 162 LNGC accidents* [39], see Figure 4.

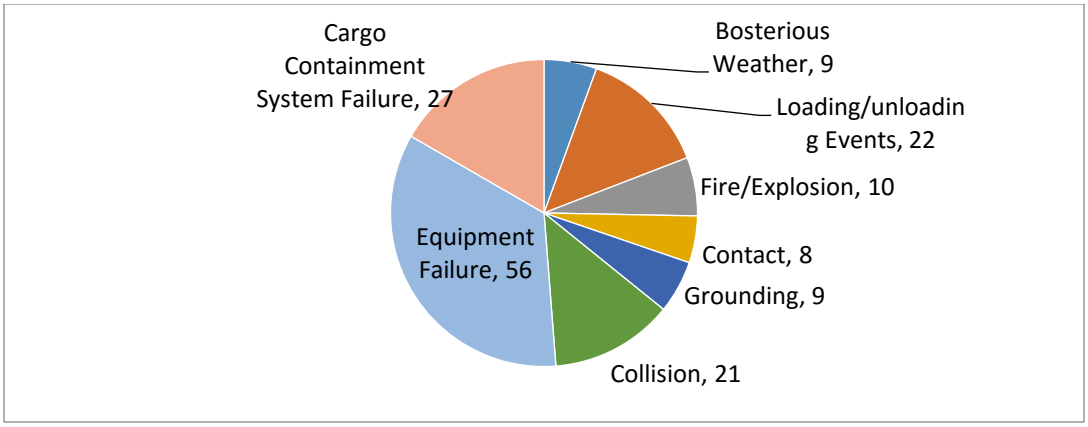

Figure 4. LNGC Accident Category Distribution

*Sources from Houston Law Center, IZAR, Colton Company, DNV report: LNG Accident review and www.seasearcher.com

To establish the LNG-FSRU location evaluation criteria, several factors, such as hydrographic information, navigation safety, fire and explosive risks, exclusion areas, and environment sensitivity, should be taken into consideration individually. Combined with previously recorded incidents, the most threaten hazards, collision, stranding, fire/explosion, and spillage during cargo handling, are selected as evaluation factors of hazard layer in the QMFMADA framework.

From Woodward et al. 2010, the potential fatalities from LNGC operations were estimated as shown in following table.

Table 1. Potential Fatalities for Major LNGC Accident Categories by Woodward 2010 [9]

Accident Category	Potential Fatalities per Year
Collision	$4.42*10^{-3}$
Grounding	$2.93*10^{-3}$
Contact	$1.46*10^{-3}$
Fire & Explosion	$6.72*10^{-4}$
Loading/Unloading Events	$2.64*10^{-4}$

From Table 1, the collision and grounding are the two most severe accidents for LNGC navigation at sea and the contacting usually happened in the harbor areas, leading to third potential fatalities among all accidents. In addition, fire/explosion and loading events should be taken more attention during LNG transferring from LNG carrier to LNG terminal. Therefore, the three processes should be evaluated individually in a quantitative way.

2.2 LNGC Navigational Process

Based on previous research experience, cargo release, collision and grounding are usually considered as major consequences of site specific risk assessment in nautical safety study. As above table mentioned, collision and grounding are selected as the major hazards for LNGC navigation safety phase.

2.2.1 Collision Model

Fujii's Model

Researcher Fujii proposed a model to calculate the average number of evasive actions (e.a.) by one ship navigating in one area. Fujii's Model is [10]:

$$\text{No.(e.a.)} = \int_{\text{entrance}}^{\text{exit}} (\rho D_e V_{rel}/V)\, dx \quad (1)$$

ρ: Traffic density, number of ships per unit area

D_e: Diameter of collision avoidance

V: Speed of passing vessel

V_{rel}: Relative speed

The value of D_e varies from 9.5 to 16.3 times of ship length, which made the collision avoidance quite conservative since the minimum shipping distance in some narrow straits are around 3 times of ship' length overall in the real world.

Macduff's Model

Another researcher, Macduff, firstly proposed the probable collision model, and the formula is [11]:

$$P = Pg * Pc \quad (2)$$

Where

-P: the probability that a vessel is involved in a collision accident during its voyage passing one assigned water area

-Pg: the geometrical probability, collision probability without aversive measures are made.

-Pc: the causation probability, the conditional probability that a collision occurs in an accidental scenario.

Pg is relevant to geometric parameters of water area, vessel size, traffic volume, course and speed; while Pg is related to mariner's skills, vessel maneuverability under accident scenarios, and many literatures considered it as a constant. Then for geometrical probability Pg, Macduff's Model estimated it as follows [11].

$$Pg = \frac{X \cdot L}{D^2} \cdot \frac{\mathrm{Sin}(\theta/_2)}{925} \tag{3}$$

Where

-D: Average distance between ships

-X: Actual length of path for one ship

-L: Average vessel length

-V: Ship's approaching speed, two ships are assumed equal

-θ: The angle that one single ship approaching the channel with

The value of Pg will be overestimated when θ is small. The assumption of two ships' speed being equal made the Pg underestimated.

Pedersen's Model

To determine the geometrical probability Pg, Pedersen and his research fellows presented a model under a two-channel situation. Channel 1 and channel 2 are assumed as two crossing channels. The equation 4 shows the Pedersen's collision model [12].

$$P_{\Delta t} = \frac{Q_j^{(2)}}{V_j^{(2)}} f_j^2(z_j) D_{ij} V_{ij} dz_j \Delta t \tag{4}$$

-Q_j: Number of movements of ship class j per unit time, named as traffic volume

-Z: Distance from the centerline of the fairway

-f: Lateral distribution of the ship routes, often normal distribution

-V_{ij}: Relative velocity; -D_i, Collision diameter

This model is reasonable for crossing scenario to estimate the geometrical probability due to a more practical assumption. However, the lack of ship movement data made it difficult to determine the probability distribution of ship motion.

In summary, Table 2 shows the expressions and characteristics of each model.

Table 2. Summary of Ship Collision Model

Model	Expression	Drawbacks
Fujii's Model	$\text{No.} = \int_{\text{entrance}}^{\text{exit}} (\rho D_e V_{rel}/V)\, dx$	De is conservative (9.5 to 16.3 times ship length), so Pg is overestimated.
Macduff's Model	$Pg = \frac{X \cdot L}{D^2} \cdot \frac{\text{Sin}(\theta/2)}{925}$	Pg is overestimated when ϴ is small and underestimated because of the assumption of two ships are equal speed.
Pedersen's Model	$P_{\Delta t} = \frac{Q_j^{(2)}}{V_j^{(2)}} f_j^2(z_j) D_{ij} V_{ij} dz_j \Delta t$	Applicable for crossing channel situation, assume ship lateral motion as normal distribution, not very accurate for head on situation

COWI Model

In order to precisely simulate the head on situation (See Figure 5) in real world, the COWI model is applied to calculate ship collision probability [13].

$$Px = Pt \times Pg \times Pc \times k_{RR} = LN_1N_2 \left|\frac{V_1 - V_2}{V_1 V_2}\right| \times \left(\frac{B_1 + B_2}{c}\right) \times (3 \times 10^{-4}) \times k_{RR} \qquad (5)$$

L: length of route segment

N_1, N_2: Number of ship 1, 2 passing per year

V_1, V_2: Speed of Ship 1 and Ship 2

B1, B2: Breadth of Ship 1 and Ship 2

Pc: Causation probability, taken as a constant 3×10^{-4}

k_{RR}: Risk reduction factor, usually taken 0.5 [13]

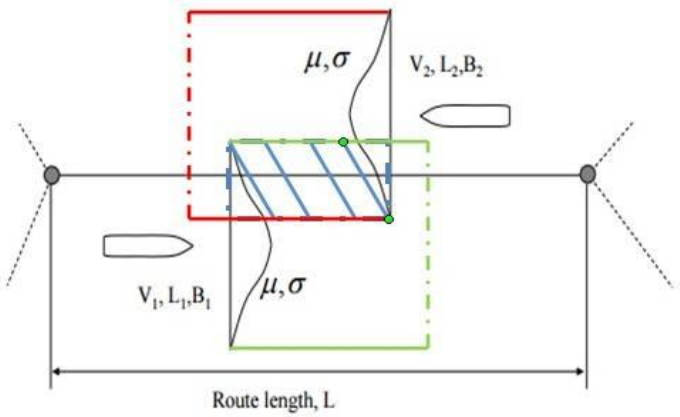

Figure 5. Head-on Collision Situation for Two Ships by Li et al., 2012 (Adapted from [13])

As shown in above figure, the overlap area was deemed as the possible collision area with the presupposition of ships' motion following normal distribution. Compared to other models, the COWI model considered the risk mitigation measure and reduced the uncertainty in some extent by assuming ship motion as normal distribution. Moreover, the most likelihood situation for LNGC navigation in inbound channel is head

on situation, so the COWI model was adopted to carry out simulation for LNGC navigation safety phase. It is widely accepted that visibility is a key factor to influence coastal navigation and the leeway and drift angle, which was deemed as a significant parameter to show the vessel's maneuverability, was largely dependent on the magnitude of wind and current. Therefore, the main parameters to evaluate the collision hazard are determined as wind, visibility and the probability of following current.

2.2.2 Grounding Model

LNGC may suffer from grounding or standing risk when it navigates without sufficient water depth and this risk may bring severe consequence if the sediment of the grounding place is considerably solid. In practice, deck officers should check the water depth reading frequently to make sure the ship has no chance to rush into the shoal when the ship is navigating in harbor areas. The following models are common ones to simulate ship's grounding.

Fujii's Model

Similarly, the concepts of geometrical and causation probability were brought to estimate likelihood of grounding as well. Fujii proposed the expected number of groundings (Ng), shown in Equation 6 [10].

$$N_G = P_C D_\rho V \tag{6}$$

Where

-Pc: Causation Probability

-V: Ship's speed

-ρ: Traffic Density

-D: The width of shoal

Macduff's Model

Meanwhile, Macduff adopted Buffon's needle problem to estimate Pg, the equation 7 shows the relationship among Pg, channel width and stopping distance of ships [11].

$$P_G = \frac{4T}{\pi C} \tag{7}$$

-C: The width of the channel

-T: The ship's stopping distance

These two above-mentioned models are only affected by the ship particulars and other elements related to location are set to be constant. The uncertainties of the real navigation situation are ignored in most cases, and this model merely considered historical accident data. But this model has been widely used as a basis to improve grounding model.

Pedersen and Simonsen's Model

Pedersen and Simonsen developed their model to estimate the expected annual number of groundings (Ng), see equation 8 [14].

$$N_G = \sum_{\text{Ship class i}}^{\text{n class}} P_{C,i} Q_i e^{-d/a_i} \int_{Z_{min}}^{Z_{max}} f_i(z)dz \tag{8}$$

Where

-Pc: Causation probability

-Q: number of transshipment per year

-a: the average time interval of position checks by deck officers

-d: the width of channel

-f(): the actual traffic distribution of ships

-z: the transverse coordinates of shoals

Table 3 serves a review of above mentioned grounding models, illustrating their expressions and drawbacks.

Table 3. Summary of Ship Grounding Model

Model	Expression	Drawbacks
Fujii's Model	$N_G = P_C D_\rho V$	Human factors, ship's maneuverability and environmental aspects were all neglected.
Macduff's Model	$P_G = \frac{4T}{\pi C}$	Causation probabilities are unknown; this model cannot recommend any risk control option. Traffic density is assumed uniformly.
Pedersen and Simonsen's model	$\sum_{\text{Ship class i}}^{\text{n class}} P_{C,i} Q_i e^{-d/a_i} \int_{z_{min}}^{z_{max}} f_i(z)dz$	Human factors and ship maneuverability are still neglected and effect of traffic (Q) and ship class (i) are not evidence based.

Montewka's Model

To overcome those above-mentioned drawbacks, Montewka et al. [15] have proposed a more accurate grounding model with the consideration of the maneuverability of an individual ship and the properties of the traffic. In addition,

Automatic Information System was employed to determine the distribution of the ship's motion.

$$F = M \times \frac{UKC}{H \times r} = \frac{R \times b}{d \times s \times c} \times \frac{UKC}{H \times r} \quad (9)$$

-F: threatened Level

-R: radius of Turning Circle

-b: a coefficient that represents the extent of damage to a ship's hull that occurs when the ship runs aground

-d: a coefficient that represents the distance at which a hazard can be detected

-s: a coefficient that represents the accuracy of depth soundings

-c: a coefficient that represents positional accuracy

-UKC: under keel clearance

-H: depth of the channel

-1/r: distance decay curve

For the LNGC navigation process, the Montewka's Model was selected as the one to simulate stranding situations since it has a better interpretation and has considered ship maneuverability. Based on the equation 9, the main parameters selected for grounding hazard of navigational process are channel width, channel curvature and under keel clearance.

2.3 Berthing Process

When berthing or unberthing operation is taking place, the LNGC shows a characteristic of low speed and large drift angle [16]. Typically, berthing operation for large ships should consider factors such as temperature, berthing ability, wind force, visibility and thunderstorm [17], another researcher Bai presented the berthing influence factors as tug assistance, wind, current, longitudinal speed control, transverse speed control and angular velocity control [18]. What is more, poor communication between crew and marine pilots during berthing operation will probably lead to marine disasters near ports, and the language and cultural diversity of seafarers needs to be considered as well [19].

To evaluate this complicated operation process in a quantitative way, Yang proposed a berthing model by presenting models of ship, propeller and rudder individually and he took full considerations of interactions between each part. As shown in Figure 6, Yang set up two coordinate systems, one is fixed coordinate X_0Y_0, and the other is ship moving coordinate system xGy [16].

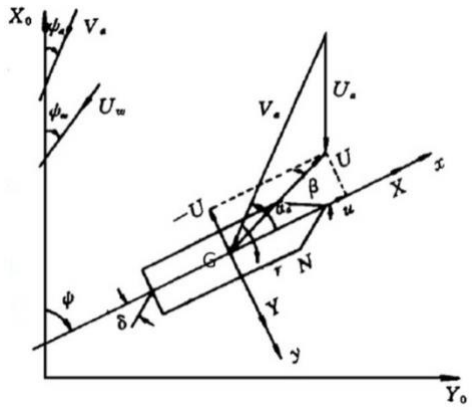

Figure 6. Two Coordinate System of LNGC by Yansheng, 1996 (Adapted from [16])

Where

-m, -m_x, -m_y: ship mass, added mass along x axis, added mass along y axis

-u, -v: line velocity components

-r: heading angular velocity

-I_{zz}: inertia moment

-J_{zz}: added inertia moment

-X, -Y: external force along X and Y axis

-N: moment of external force

-H: ship hull; -P: propeller; -R: rudder; -A: wind; -L: mooring line; -C: anchor; -S: bank wall; -T: tug.

Based on the above-mentioned theory, LNG ship simulator DMU V-Dragon 3000A was employed to perform a high-precise simulation for LNGC berthing. This simulator adopted a six -freedom motion mathematical model and integrated wind

disturbing force model (Equ. 10, 11, 12) and wave force model (Equ. 13, 14, 15) as the key ones for external force [20].

Wave Disturbance Model

$$X_A = \frac{1}{2}\rho_A A_f U_R^2 C_{X_a}(\alpha_R) \tag{10}$$

$$Y_A = \frac{1}{2}\rho_A A_s U_R^2 C_{Y_a}(\alpha_R) \tag{11}$$

$$N_A = \frac{1}{2}\rho_A A_s L_{oa} U_R^2 C_{N_a}(\alpha_R) \tag{12}$$

-Cxa(αR), -Cya(αR), -Cna(αR): wind pressure coefficients

-As: Lateral projection area at waterline

-Af: Conformal projection area at waterline

Secondary Order Wave Force Model

$$X_{W_2} = \frac{1}{2}\rho L a^2 \cos(\chi)\, C_{XW}(\lambda) \tag{13}$$

$$Y_{W_2} = \frac{1}{2}\rho L a^2 \sin(\chi)\, C_{YW}(\lambda) \tag{14}$$

$$N_{W_2} = \frac{1}{2}\rho L^2 a^2 \sin(\chi)\, C_{NW}(\lambda) \tag{15}$$

Where

-Cxw(λ), -Cyw(λ), -Cnw(λ): experiment coefficients

-a: wave amplitude

-χ: wave direction angle

-λ: wave length

To evaluate the LNGC berthing operation, six main parameters were determined by the equations 10-15, they are : water depth of turning basin, following current speed,

berth length, radius of turning area, transverse wave height and the probability of crossing wind (beam wind).

2.4 LNG Transferring Process

After the berthing process is completed, the LNG should be transferred from LNGC to LNG FSRU, which is a typical Ship to Ship LNG transferring process. Two common solutions for Ship to Ship transferring process, one is called side-by-side transferring pattern, and the other is called tandem transferring pattern [21]. There are three liquid transferring connection hoses and one vapor counterflow connection hose in the Figure 7.

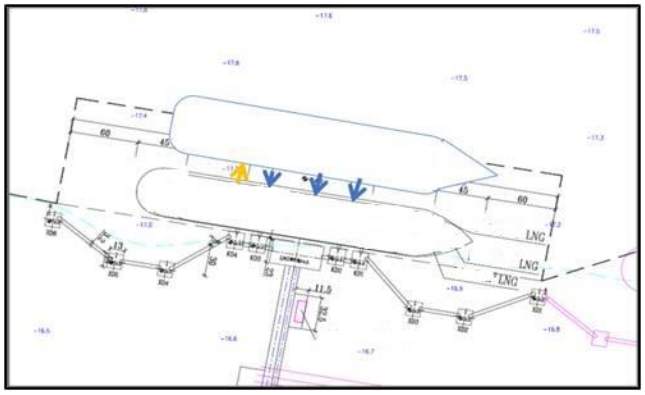

Figure 7. Ship to Ship Pattern for LNG FSRU System

Besides the preparation work prior to transferring operation, the typical STS process should include: mooring to the FSRU, water curtain switch on, connecting

transferring hose, inerting of LNG fuel hose and transferring arm, cool down transferring hose, oxygen test, leak test, Emergency Shut Down System (ESDS) test under normal and low temperature, leakage and temperature monitoring during transferring, and post processing actions such as draining, methane purging for liquid line and vapor line, measurement after transfer and transferring hose disconnection [22].

For the LNG FSRU system, many causes would result in LNG accidental release such as FSRU or LNGC tank breach, connection pipe rupture and LNG vaporizer failure. Furthermore, possible associated consequences of LNGC release on water have been identified as BLEVE, vapor cloud explosion (VCE), jet fire, flash fire, pool fire, RPT, cryogenic burns, etc. Figure 8 shows a simplified bow-tie diagram for LNG accidental release to consider both the causes and the outputs of the top event [5, 9, 23].

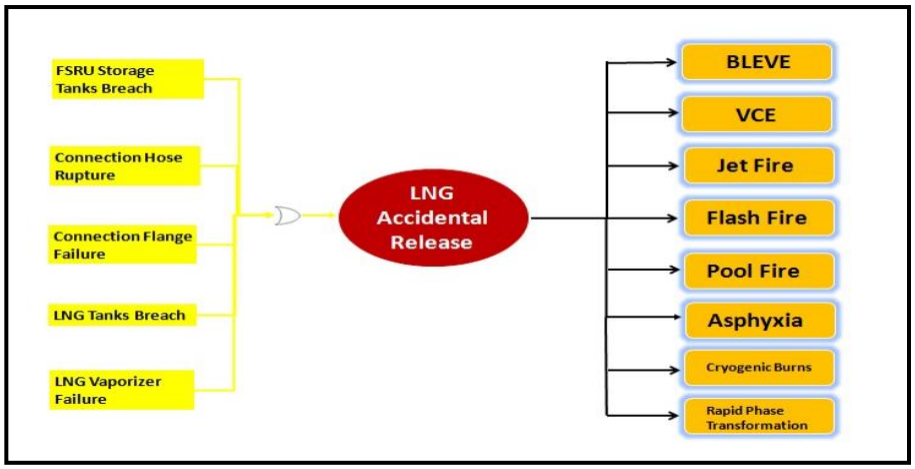

Figure 8. Bow-tie Diagram for LNG Accidental Release

As shown in above bow-tie diagram, five causes may result in LNG accidental release for the LNG FSRU system: FSRU storage tank breach, connection hose rupture, connection flange failure, LNG Tank breach and LNG vaporizer failure. To simulate the most probable leading factors of LNG transferring process, two events, connection hose rupture and connection flange failure, were identified as a result of their high-risk characteristic. During LNG transferring process, the accidental release of LNG could lead to many possible consequences. When LNG is released under the waterline, it may probably convert to vapor bubble, then LNG bubble may escape above the waterline to produce LNG vapor. For above-waterline release, jet fire, flash fire and pool fire may form under different scenarios. The following figure is the event tree analysis for LNG accidental release [9, 24, 25, 31].

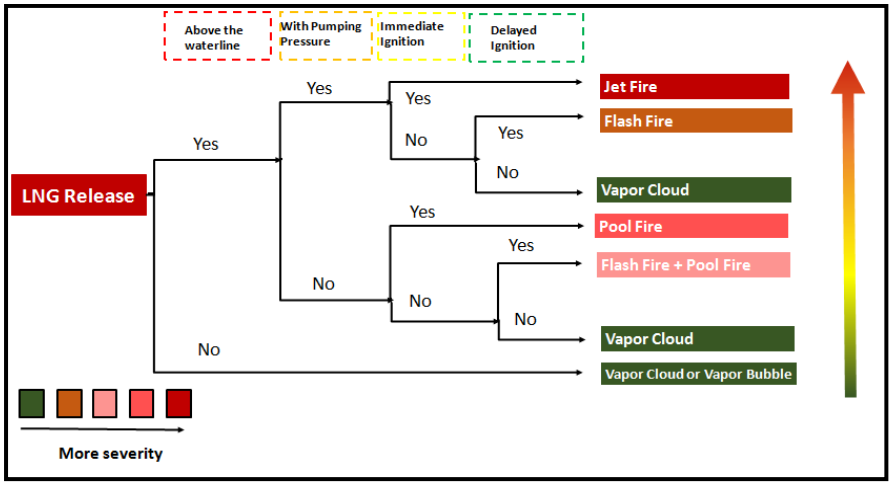

Figure 9. Event Tree Analysis for LNG Release

As above mentioned, events of connection hose rupture and connection flange failure were identified to list on the hazard layer of the final framework. In addition, as shown in Figure 9, the possible fatality related consequences are flash fire, pool fire and jet fire, since the explosion is not likely to occur in the open water area [26, 31].

After the two events and relevant consequences were identified, the dispersion models and the fire models were needed to process flammable calculations. The flammable calculations include fireballs (instantaneous releases), jet fires (pressurized releases), pool fires (after rainout), and vapor cloud fires or explosion. This study adopted the Unified Dispersion Model (UDM) as the core model to research the dispersion effects of LNG releasing on water, which is also widely applied in the hazard assessment software package Phast and Safeti [42].

2.4.1 Dispersion model

In this research, crosswind situation was selected as a risk-seeking scenario to evaluate the LNG FSRU system. To simulate crosswind situation, three consecutive phases were adopted for two scenarios which were instantaneous release and continuous release.

Phase 1, Jet Spreading

The cloud is assumed to remain circular until the passive transition or until the spread rate reduces to the heavy-gas spread rate, [42]

$$R_y = R_z \tag{16}$$

Where

-Ry and -Rz are the ellipse semi-axes.

Phase 2, Heavy-gas Spreading

After the jet spreading phase, the heavy-gas spreading phase served as the second one.

For instantaneous dispersion,

$$\frac{d\,R_y}{dt} = \frac{C_E}{C_m}\sqrt{\frac{g\{\max[0,\rho_{cld}-\rho_a(z=z_{cld})]\}H_{eff}(1+h_d)}{\rho_{cld}}},\ C_m = [\Gamma\left(1+\frac{2}{m}\right)]^{1/2} \qquad (17)$$

For continuous dispersion,

$$\frac{d\,R_y}{dx} = \frac{C_E}{u_x C_m}\sqrt{\frac{g\{\max[0,\rho_{cld}-\rho_a(z=z_{cld})]\}H_{eff}(1+h_d)}{\rho_{cld}}},\ C_m = \Gamma\left(1+\frac{1}{m}\right) \qquad (18)$$

Where

-C_m = 1.15, Van Ulden cross-wind spreading parameter

-H_{eff}: effective height of cloud after full touchdown

-h_d: fraction of bottom half of cloud which is above ground

-C_m: conversion factor between cloud half-widths

-C_E: parameter in gravity-spreading law

-m: exponent of horizontal distribution function for concentration

-ρ_a: density of ambient air

- ρ_{cld}: density of plume

-u_x: horizontal component of cloud speed

-z: vertical height above ground

-z_{cld}: height above ground of cloud centerline

Phase 3, Passive Spreading

After the jet spreading and heavy-gas spreading, the passive spreading was applied, and the equations are as follows [42].

$$\frac{d\,R_y}{dt}[at\ x] = u_x\sqrt{2}\frac{d\,\sigma_{ya}}{dx}[at\ x - x_0] \quad \text{instantaneous} \tag{19}$$

$$\frac{d\,R_y}{dx}[at\ x] = \sqrt{2}\frac{d\,\sigma_{ya}}{dx}[at\ x - x_0] \quad \text{continuous} \tag{20}$$

Where

-x: horizontal downwind distance

-σ_{ya}: standard empirical correlation for passive crosswind dispersion coefficient

2.4.2 Fire Model

Typically, there are three types of fires related to LNG spillage on the water, jet fire, pool fire and flash fire.

The jet fire in this research was produced by a liquefied/ two phase natural gas. The effective source diameter of the flame is significant to correctly simulate the effect zone of jet fire. The following equation is the expression of effective source diameter (Ds) [55].

$$D_s = 2r_j\sqrt{\frac{\rho_j}{\rho_{vap}[T_{sat}(P_o)]}} \tag{21}$$

Where

-rj: expanded radius of the escaping fluid

-Po: atmospheric pressure

- $\rho_{vap}[T_{sat}(P_o)]$: the saturated vapor density of the fuel at ambient pressure

- ρ_j: Density of expanded fluid jet

Besides jet fire, pool fire is another possible fire type when releasing on the water. To determine the magnitude of the surface emissive power of pool fire, the following equation is adopted [56].

$$E_f = E_m \left[1 - e^{-\frac{D}{L_s}}\right] (Luminius\ Fires) = E_m \left[e^{-\frac{D}{L_s}}\right] + E_s \left[1 - e^{-\frac{D}{L_s}}\right] (\text{Sooty Fires}) = \frac{\chi_R m \Delta H_c}{[1+4\frac{H}{D}]} (General\ Fires) \quad (22)$$

Where,

-Em: Maximum emissive power for luminous fires

-Es: Smoke emissive power

-Ls: A characteristic length for decay of surface emissive power

-χ_R: The ratio of the total energy radiated to the total energy released

-D: Diameter of the flame

-H: Height of the flame

The equation for "general fires" was applied when the experimental data were not available.

CHAPTER III

METHODOLOGY AND FRAMEWORK DEVELOPMENT

To establish the evaluation framework as shown in Figure 1, the layers should be determined from top to bottom. The second layer is filled with three processes defined in chapter I: LNGC Navigation Process, Berthing Process and LNG Transferring Process. Then the third layer, identified hazard layer, was determined by chapter II.

3.1 Framework Development

For the navigational process, collision and grounding are the major hazards for LNGC, and from Equation 5, visibility, wind and current are the attributes to lead to collision. Similarly, the major parameters in Equation 9, *i.e.,* UKC, Channel Width and Channel Curvature, are the attributes to result in LNGC aground.

For berthing process, DMU ship simulator was adopted to analyze the attributes. The extreme conditions were selected as the input parameters: the wind direction was blowing to the shore, North; the radius of turning area was set as 500 meter and 1000 meter, respectively; the berthing length was set 1.2 times and 2 times ship's length overall; and other values of parameters were obtained when the incident happened. Two scenarios were designed to determine the most influential factors:

1. Full loaded, port side berthing with spring tidal current;
2. Full loaded, starboard side berthing with ebbing tidal current.

The failure simulation runs were shown in Table 4.The major consequences of berthing process were contacting with obstruction and collision with the FSRU, the offshore “pier”.

Table 4. Simulation Results of Ship Simulator for Berthing Process

Number of runs	Wind	Current	Radius of Turning Area	Water Depth	Transverse Wave Height	Berth Length	Consequence
1	N-6	Spring, 0.6m/s	**500m**	20m	0.7m	2L	Contacting the FSRU
2	N-6	**Spring, 1.5m/s**	1000m	21m	0.8m	2L	Contacting the jetty nearby
3	**N-8**	Spring, 0.8m/s	1000m	21m	1.0m	2L	Contacting the FSRU, tugs malfunction
4	N-6	Spring, 0.6m/s	1000m	19m	**1.5m**	2L	Contacting the berthing ship nearby
5	**N-8**	Ebb, 0.9m/s	1000m	20m	0.8m	2L	Contacting the FSRU, tugs malfunction
6	N-7	Ebb, 0.7m/s	1000m	**15m**	0.8m	2L	Contacting with the berth nearby
7	N-6	Ebb, 0.6m/s	1000m	20m	0.7m	**1.2L**	Contacting with FSRU, failed to get alongside the berth
8	N-6	Spring, 0.6m/s	1000m	20m	0.8m	**1.2L**	Contacting with FSRU, failed to get alongside the berth

Based on the simulation results by DMU V-Dragon 3000A ship simulator, the most significant parameters leading to LNGC contacting with the nearest obstruction are water depth in that area, transverse wave height of turning area and the magnitude of following current; while the attributes for contacting between LNGC and LNG FSRU are berth length, radius of turning basin area and the probability of crossing wind.

For LNG transferring process, vapor cloud, pool fire, flash fire and jet fire may be the outputs of the connection flange failure and connection hose failure. Therefore, the final framework of QMFMADA is established accordingly, see Figure 10.

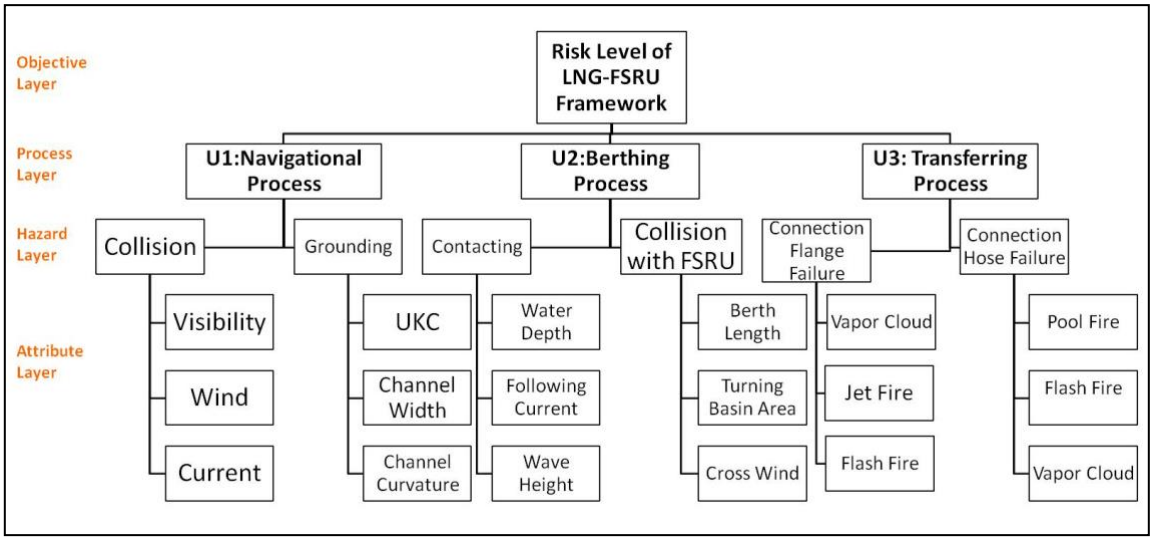

Figure 10. LNG FSRU System Evaluation Framework of QMFMADA

3.2 Parameters Determination

After the final framework was determined by adopting a top-to-bottom strategy, the evaluation work can be processed from an adverse way, attribute layer goes first. In this study, the whole LNG FSRU system comprised one LNG carrier, one LNG floating receiving terminal and the interact operation between them. So, the characteristics of LNGC and LNG FSRU should be determined as a preparation work. Recent years, two most common large-scale LNG ship type, Q-Flex and Q-Max, were widely used all over world for LNG long distance transiting. To consider the current trend for LNG offshore application, Q-Flex was applied in this study as the input ship type of ship simulator DMU V-Dragon 3000A, and the dimension of its receiving terminal FSRU was employed accordingly [27], see Table 5.

Table 5. Parameters of LNGC and FSRU

Parameters	LNGC(Q-Flex)	FSRU
LOA	303	315
Loading Capacity	142933.7 m^3	217000 m^3
Breadth	50	50
Draft	12	12.5

Referred from the previous reports, the loading / unloading equipment of FSRU have 4 liquid loading hoses and 2 vapor return hoses, each of them has one spare part.

The maximum loading capacity, length of LNG loading hoses and other parameters are listed in Table 6 [28].

Table 6. Parameters of FSRU's Loading Equipment [28]

Parameter	Value
Maximum Loading Capacity	8000 m^3/h for all loading hoses
Maximum Unloading Capacity	5000 m^3/h for all loading hoses
Number of LNG Loading Hoses	4 (1 spare)
Number of Vapor Return Hoses	2 (1 spare)
Inner Diameter of LNG Loading Hoses	0.254 m
Length for LNG Loading Hoses	18.5 m
Inner Diameter of LNG Loading Hose Flange	0.41 m
Inner Diameter of Vapor Return Hose Flange	0.41 m

As shown in Table 6, the value of maximum loading capacity will be applied to determine the estimated release volume and the diameter of LNG loading hoses and loading hose flange were utilized as the key factors to define scenarios for consequence analysis in the following chapters.

CHAPTER IV

CASE STUDY FOR DEFINED SYSTEM

To find out a favorable position to build LNG FSRU system, two locations from China were applied to carry out case study based on the proposed framework. One location is New Port of Dalian, northern part of China; the second one is Qidong Port of Nantong, the East China Sea, shown in Figure 11.

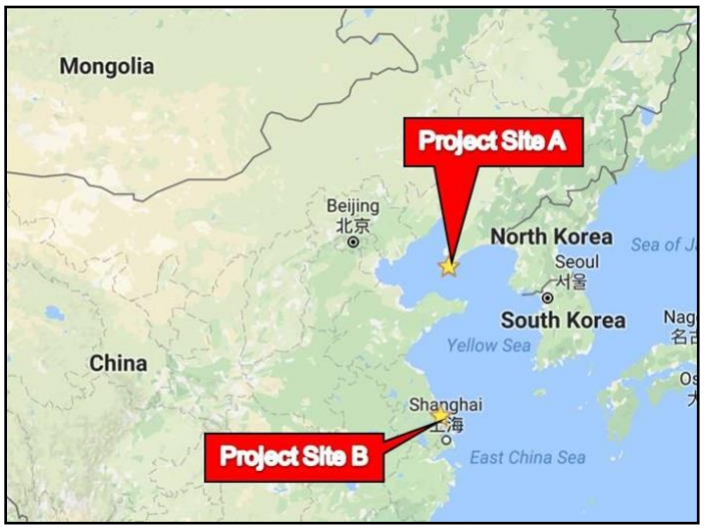

Figure 11. Two Alternative Locations for LNG FSRU System

The proposed LNG FSRU layout maps of two locations were drawn in Figure 12. The proposed LNG FSRU for Dalian locates at the south edge of the coast line while the

proposed one for Nantong locates at the northeast side of the coast line. The harbor layout maps of two locations were shown in Figure 12 by Google Map.

Figure 12. Harbor Layout Maps for Two Alternative Locations

The yellow arrows in Figure 12 showed the exact positions for the LNG FSRU. The proposed direction of location A is 053° ~ 233°, berth length is 446 meters (m); the design direction of location B is 099° ~ 279° and berth length is 430 m. Figure 13 showed the parametric design for two locations by Auto CAD.

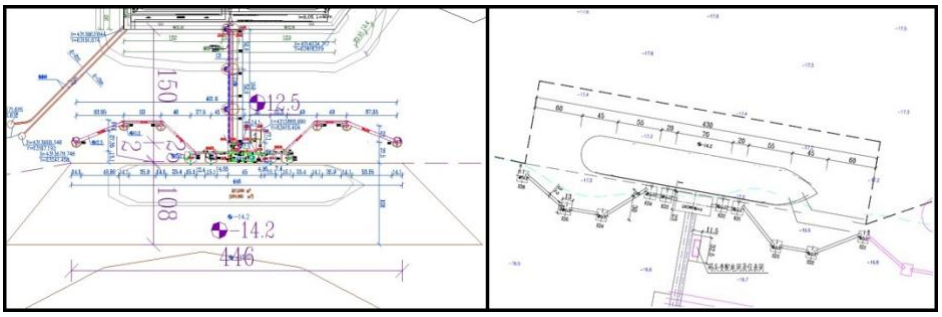

Figure 13. LNG FSRU Layout Maps of Two Locations

After the dimension of two proposed locations were determined, the evaluation steps can be processed from LNGC navigating in the inbound channel to the LNG successfully transferring from LNGC to LNG FSRU.

4.1 Data Collection for Navigational Process

The left side figure is the layout map of location A (Dalian proposed LNG FSRU), while the right one is the layout map of location B (Nantong proposed LNG FSRU). To evaluate the framework of QMFMADA, the bottom-to-top sequence should be adopted, so the factors of very bottom attribute layer for navigation process are visibility, wind and current.

Considering the data availability for attributes of collision hazard, the visibility parameter is determined by number of days under poor visibility (visible distance < 4000m) per year; the wind parameter is determined by Number of days under standard wind scale, which is equal to number of days under Beaufort scale 6 and 7 plus 1.5 times number of days under Beaufort scale 8 or more [29]; and the parameter current is determined by the probability of following current, which is the most difficult situation for ship maneuvering. For grounding hazard, the attribute channel width and channel curvature can be determined directly by the actual channel data, and the minimum under keel clearance (UKC) is equal to the minimum chart water depth minus actual draft of LNGC. The actual values of navigation process related attributes for two alternatives are shown in Table 7.

Table 7. Values of Navigational Process Related Attributes for Two Locations

	Channel Width	Channel Curvature	UKC	Windy Days	Following Current Prob.	Visibility
Location A	1050m	31°	12m	140	7.6%	22
Location B	690 m	27°	5m	151	9.3%	30

Referred from the Code for Design of Liquefied Natural Gas Port and Jetty [30], the limited conditions for ship's navigating in channel were regulated as follows.

Wind speed should not exceed 20m/s and the transverse waves should be less than 2.0 meters, while the magnitude of following waves should not exceed 3.0 m; Visibility for LNGC navigating in the inbound channel should be greater than 2000 meters and the upper limit for transverse speed of current is 1.5 m/s, while the following current speed should not exceed 2.5 m/s.

4.2 Data Collection for Berthing Process

For the second process, berthing process simulation, the water depth for the contacting possibility for LNGC and other navigation obstruction is the minimum water depth in berthing area; "Following Current" is the magnitude of following current during berthing operation; while the transverse wave height can be directly obtained from the hydrographic data of two harbor authorities. For the hazard of possible collision with FSRU, the berth length and turning basin area is the values of designed berth length and radius of turning water shown in Figure 12, and the crossing wind, which is defined as

the wind blowing the LNGC toward FSRU side, was evaluated by the wind rose maps of two locations. Therefore, the values of berthing process related attributes are shown in Table 8.

Table 8. Values of Berthing Process Related Attributes for Two Locations

	Water Depth	Following Current	Wave Height	Berth Length	Radius of Turning Area	Crossing Wind Prob.
Location A	20 m	0.8m/s	1.08 m	1.5L	1020m	4.6%
Location B	17m	0.85m/s	0.81 m	1.25L	1260m	3.8%

In addition, the Code for Design of Liquefied Natural Gas Port and Jetty [30] was referred to adjust the environmental input data for berthing process simulation. The code regulated berthing limited conditions as follows: The maximum allowable wind speed should be 15 m/s; The transverse waves should not exceed 1.2 meters, while the threshold value of following waves should be 1.5 m; Visibility for navigating in the inbound channel should be greater than 1000 meters; The upper limit for transverse current speed is 0.5 m/s, while the following current speed should not exceed 1.0 m/s.

4.3 LNG Transferring Process Simulation

After the LNGC is safely getting alongside the LNG FSRU, the system moves to the last stage, LNG transferring from LNGC to FSRU.

4.3.1 Defined Scenarios

Based on the previous research [32, 33, 34], it is a reasonable to simulate this event “LNG releasing on the water” by two scenarios: one is called maximum credible scenario (MCS), which is the most possible scenario for one year the LNG FSRU system may face; another one is called worst case scenario (WCS), which means the extremely dangerous situation for LNG FSRU system [35].

To process the simulation by Safeti 7.2, several input parameters should be determined. For the two scenarios, the external environment factors for weather data input, wind, air temperature and relative humidity, can be obtained from the meteorological and hydrographic records of two locations.

For maximum credible scenario, the input parameter “wind” was the prevailing wind for two locations. As shown in Figure 14, the wind rose map of location A shows the prevailing wind direction was north wind with the speed of 8 m/s; while the prevailing wind direction of location B is northeast wind with the speed of 6.7 m/s; the air temperature for MCS was the average temperature of one whole year, where 10.5 degree centigrade for location A and 15.1℃ for location B; similarly, the humidity parameter was selected as the average humidity for a whole year, 69% for location A and 75% for location B.

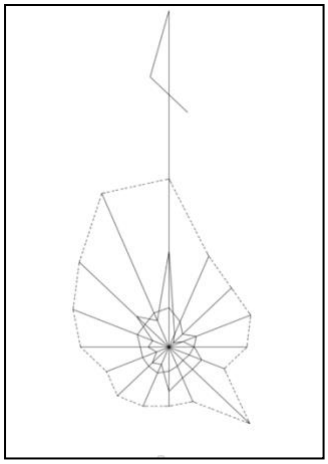

Figure 14. Wind Rose Map of Location A (Adapted from [57])

Table 9. Wind Direction Frequency Distribution (Adapted from [57])

	Average Speed (m/s)	Max. Speed (m/s)	Frequency (%)
N	8.0	34.2	19.5
NNE	5.6	20.0	2.8
NE	3.7	17.0	1.2
ENE	5.7	17.0	2.9
E	4.8	15.0	4.9
ESE	4.2	11.5	6.8
SE	3.8	22.0	6.4
SSE	4.2	12.0	6.8
S	4.9	12.0	9.0
SSW	5.7	13.0	3.8
SW	5.5	14.0	4.5
WSW	5.5	13.0	2.6
W	5.5	17.0	4.0
WNW	6.6	20.0	3.4
NW	6.5	24.4	8.8
NNW	7.5	33.8	5.8
CALM			6.8

For worst case scenario, the “wind” parameter was the most hazardous when the wind is blowing toward the pier since the fire may get more assets and people involved.

By considering the wind rose map of each location, the most hazardous wind directions were southeast and northeast for location A and location B, respectively and the worst wind speed is 15m/s because it is the maximum speed to still allow LNG transferring operation to process [30]. Since the air temperature may fluctuate day to day, the WCS air temperature was chosen as the highest monthly average one for a whole year, 15.1℃ for location A and 20.6℃ for location B. Similarly, the humidity parameter was determined as the highest monthly average humidity for a whole year, 83% for location A and 88% for location B.

The release preconditions, hose loading capacity, leakage time and hole size, were determined as the main parameters to define the exact releasing volume of MCS and WCS. For WCS, the hose loading capacity was referred as the LNG FSRU's maximum loading capacity and the accidental release time was determined as 20 minutes to calculate the simulated release volume for the events as connection hose rupture and flange failure. As shown in table 5, the inner diameter of LNG loading hose and loading hose flange were 0.254 m and 0.41 m, respectively, so the hole size was determined as the total-damage scenario. For MCS, the hose capacity was determined as the 87% of the maximum loading capacity and the release time was the 10 minutes; the holes was determined as 0.2 m for connection flange failure and 0.12 m for connection hose rupture scenario. The input data for MCS and WCS simulation are listed in Table 10.

Table 10. Input Data for Safeti Simulation Plans

	Wind	Air Temperature	Humidity	Pasquill Stability	Release Time	Hole Size Diameter
Maximum Credible Scenario (MCS)	Prevailing Wind (A; 8 m/s, N; B:6.7m/s, NE)	Yearly Average (A: 10.5℃; B:15.1℃)	Yearly Average Humidity (A: 69%; B: 75%)	E	1167 m^3	0.2m (Flange Failure)/0.12m (Hose Rupture)
Worst Case Scenario (WCS)	15m/s (A: SE; B: NE)	Highest Monthly Average Temperature (A: 15.1℃; B: 20.6℃)	Highest Monthly Average Humidity (A: 83%; B: 88%)	Loc. A: C; Loc. B: D	2667m^3	0.41 m (Flange Failure)/0.254 m (Hose Rupture)

4.3.2 Simulation Results

The runs were designed in 4 group comparisons with 8 simulations. Simulation plan 1, 2, 3 and 4 were taken for connection flange failure. Among these four simulation plans, simulation plan 1 and 2 took place in location A under scenario MCS and WCS, respectively; Simulation plan 3 and 4 took place in location B under scenario MCS and WCS. Meanwhile, simulation runs 5 to 8 were for connection hose rupture, and simulation plan 5 and 6 took place in location A under scenario MCS and WCS; Simulation plan 7 and 8 took place in location B under scenario MCS and WCS, respectively.

Figure 15 shows the preliminary simulation outputs by Safeti 7.2 for two alternatives under the condition of “flange failure with worst case scenario” (simulation plan 2 and 4).

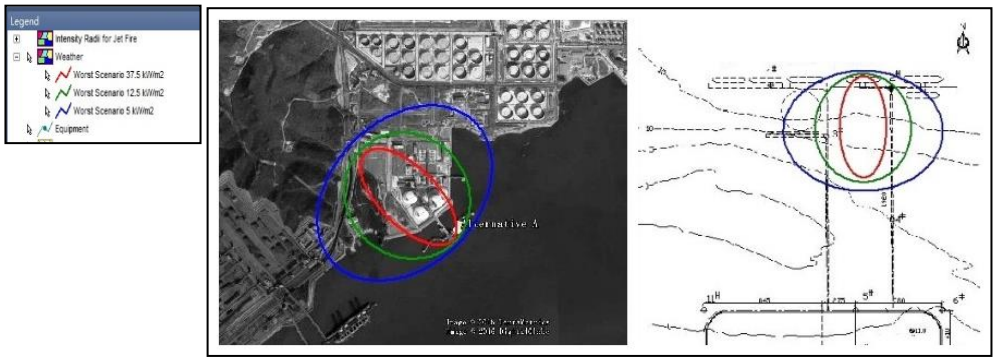

Figure 15. Simulation Outputs for Two Alternatives under WCS and Flange Failure

From Figure 15, the left one is the simulated thermal radiation influence areas of location A and the right one is that of location B. The red circle is the high thermal radiation area with heat flux 37.5 kW/m^2, the green one is the thermal radiation intensity of 12.5 kW/m^2 and the blue circle is the range of thermal radiation intensity of 5kW/ m^2. Meanwhile, other simulation plans were taken under different input data, and Table 11 shows all simulated outcomes of eight simulation plans. The potential fatalities would be calculated based on the values of thermal radiation distance and flammability limits distance in the following chapter.

Table 11. Outcomes of Designed Simulation Plans

Plan	Location	Scenario	Dia. of Hole Size (mm)	Est. Leakage Volume	Fire Type	Thermal Radiation Distance			Flammability Limits Distance		
						4kW/m^2	12.5kW/m^2	37.5kW/m^2	UFL	LFL	0.5LFL
1	A	MCS	200	1167	Flash				220	794	1590
2	A	WCS	410	2667	Jet	1141	1022	976			
3	B	MCS	200	1167	Flash				194	771	1546
4	B	WCS	410	2667	Jet	1128	1016	976			
5	A	MCS	120	1167	Flash				11	77	277
6	A	WCS	254	2667	Pool	501	302	192			
7	B	MCS	120	1167	Flash				9	70	202
8	B	WCS	254	2667	Pool	722	525	222			

CHAPTER V

EVALUATION RESULTS AND DISCUSSION

After the completion of simulation runs for three processes, the utility value should be determined from bottom hierarchy to the top. Navigational process and berthing process, which were called maritime safety study in this research, adopted risk evaluation matrix to determine each utility value; while for chemical process safety part, LNG transferring process was determined by the potential loss of life (PLL) [36].

5.1 Evaluation Methodology for Maritime Safety Study

In order to establish the relationship between expected utility value and risk level, five qualitative evaluation scales (favorable, acceptable, moderate, limited acceptable, and unacceptable) are converted to five utility ranges evenly. 90 experts were consulted to determine the evaluation standards for each attribute of navigational process and berthing process shown in Figure 10.

To avoid subjectivity, 30 senior officers of deck department aboard ships, 30 professional pilots and 30 professors from marine maneuvering major built up the expert judgment team for this research. Based on the opinions of the expert judgment team and previous studies on the marine maneuvering, every individual attribute was evaluated quantitatively based on the risk utility value (RUV) or risk tolerance index, which was

distributed evenly from 0 to 1 with the interval of 0.2. Furthermore, risk utility value range from 0.8 to 1.0 means the environment of this location is favorable to build LNG FSRU, while the value locating between 0.6 and 0.8 means it is acceptable for LNG FSRU; the range 0.4 to 0.6 means moderate environmental conditions for the system; limited acceptable when the RUV is in the range of 0.2 to 0.4; it is unacceptable when the utility value goes below 0.2 [40].The evaluation standards for adopted attributes of navigational and berthing process were established based on the questionnaires (see Appendix 1) collected from professors, pilots and senior officers onboard.

5.1.1 Evaluation Standards for Risk Utility Value

"Visibility", as an example, was determined by the number of days under poor visibility (visible distance < 4000m) per year [29, 37]. Four risk utility values (0.8, 0.6, 0.4 and 0.2) were given to experts to get their opinions on the risk standard of "visibility" to build LNG FSRU. From the collected data, Figure 10 showed the distributions of restricted visibility days per year where it is favorable/ acceptable/ moderate / limited acceptable/ unacceptable for LNG FSRU operations.

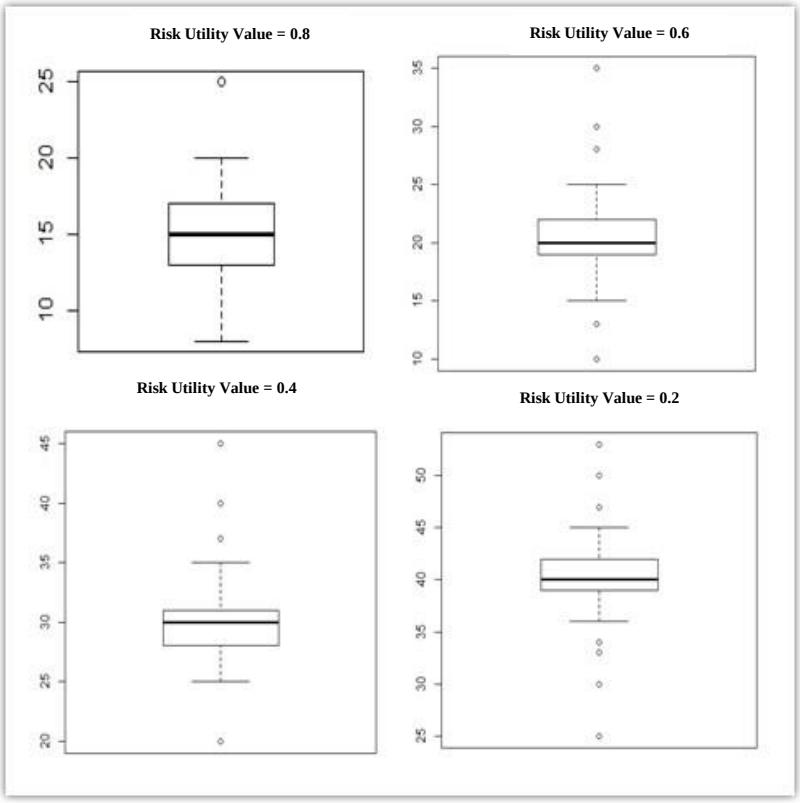

Figure 16. Data Analysis of Boundary Values of "Visibility"

Since there were some outliers among these four graphs, the new distribution without outliers can be shown on the Figure 15. Therefore, the point value of these four risk utility values with 95% confidential interval can be (14.47, 15.64), (19.68, 20.70), (29.15, 30.22) and (39.77, 40.65) with the p value much smaller than 0.05, shown in Appendix 2. Therefore, the evaluation standard for "visibility" was shown on Table 12.

Table 12. Evaluation Standard for "Visibility"

Utility / Range / Factors	Favorable, (0.8,1]	Acceptable, (0.6,0.8)	Moderate, (0.4,0.6]	Limited Acceptable, (0.2,0.4]	Unacceptable, [0,0.2]
Visibility	＜15	15 ~ 20	20 ~ 30	30 ~ 40	＞40

The total evaluation standards based were displayed in the Table 13 by analyzing the collected data for all the attributes of navigational process and berthing process.

Table 13. Evaluation Standards for Each Attribute of Maritime Safety Study

Utility / Range / Factors	Favorable, (0.8,1]	Acceptable, (0.6,0.8)	Moderate, (0.4,0.6]	Limited Acceptable, (0.2,0.4]	Unacceptable, [0,0.2]
Visibility (d/y)	＜15	15 ~ 20	20 ~ 30	30 ~ 40	＞40
Windy Days (d/y)	＜30	30 ~ 60	60 ~ 100	100 ~ 150	＞150
Following Current Prob.	< 3%	3~6%	6~10%	10~15%	>15%
Channel Width	>900	650~900	450~650	300~450	< 300
Channel Curvature	<15°	15°~25°	25°~35°	35°~45°	>45°
UKC	>15m	10~15m	5~10m	2~5m	<2m
Water Depth	>25m	22~25m	18~22m	15~18m	<15m
Following Current	<0.3m/s	0.3~0.6	0.6~0.8	0.8~1	>1m/s
Wave Height	＜0.3m	0.3 ~ 0.6	0.6 ~ 1.0	1.0 ~ 1.2	＞1.2m
Berth Length	>2.5L	2~2.5L	1.5~2L	1.2~1.5L	<1.2L
Turning Basin Area	>1200m	1000~1200 m	800~1000 m	600~800 m	<600m
Cross Wind Prob.	< 1.5%	1.5~3%	3~4.5%	4.5~6.5%	>6.5%

5.1.2 Risk Utility Value Analysis

To get the expected value of each attribute for both alternatives, the utility value for the bottom hierarchy should be calculated first. Ua(Collision) was taken as an example, the value of it should be calculated by attributes "visibility", "windy days" and "following current probability". Based on expert judgment records, the utility function for "visibility" can be obtained by the statistics software R.

Firstly, the total data were split into three parts, 45 data points for training data, 10 data points for validation data set and 35 data points for testing data. From the output of plot command, one outlier (Vis=45, Risk=0.6) and one leverage (Vis=125, Risk=0.05) were identified, then the new data set were established without those two data points.

Suppose the data points following linear regression, the regression function should be:

$$Risk = \beta_0+\beta_1 Vis+\ldots+\beta_n Vis^n \tag{23}$$

Five regression functions were tried for "Visibility" by R, shown in Appendix 3 (Figure 1~5). Table 14 showed all the summaries about these five regression models for "Risk ~ Visibility".

Table 14. Summary of Five Possible Regression Functions

	R Square Value	Coefficients	Comments
Risk= $\beta_0+\beta_1$Vis	0.77	$\beta_0 = 0.83$ $\beta_1 = -0.011$	The least R square value; The standard residual plot showed the linearity and heteroscedasticity were not good; The scale-location plot showed a curve with non-equally spreading residuals
Risk= $\beta_0+\beta_1$In(Vis)	0.93	$\beta_0 = 1.931$ $\beta_1 = -0.438$	The standard residual plot showed the linearity and heteroscedasticity were not good; The scale-location plot showed the residual spreading equally along the ranges of predictors; But the Cook's distance line was a broken line.
Risk= $\beta_0+\beta_1$Vis+ β_2Vis^2	0.96	$\beta_0 = 1.251$ $\beta_1 = -0.035$ $\beta_2 = 2.56*10^{-4}$	The standard residual plot showed the linearity and heteroscedasticity were good; The scale-location plot showed the residual spreading equally along the ranges of predictors; But the Cook's distance line was close to a line with one point locating between 0.5 and 1.
Risk= $\beta_0+\beta_1$Vis+ β_2Vis^2 +β_3Vis^3	0.98	$\beta_0 = 1.464$ $\beta_1 = -0.055$ $\beta_2 = 7.49*10^{-4}$ $\beta_3 = -3.44*10^{-6}$	See Figure 17.
Risk= $\beta_0+\beta_1$Vis+ β_2Vis^2+β_3Vis^3 +β_4Vis^4	0.98	$\beta_0 = 1.362$ $\beta_1 = -0.041$ $\beta_2 = 1.87*10^{-4}$ $\beta_3 = 5.34*10^{-6}$ $\beta_4 = -4.59*10^{-8}$	The largest R square value; P value of β_2, β_3 and β_2 were much larger than 0.05; The standard residual plot showed the linearity and heteroscedasticity were good; The scale-location plot showed the residual spreading equally along the ranges of predictors; But the Cook's distance line was close to a line with one point locating close to 1.

According to the column of "R-square value", the last two functions were the best among all five models as per their good interpretation for existed data points. However, interpretation and prediction should be balanced to get an optimal model by the comprehensive performances, and Figure 17 showed the performance of the fourth function.

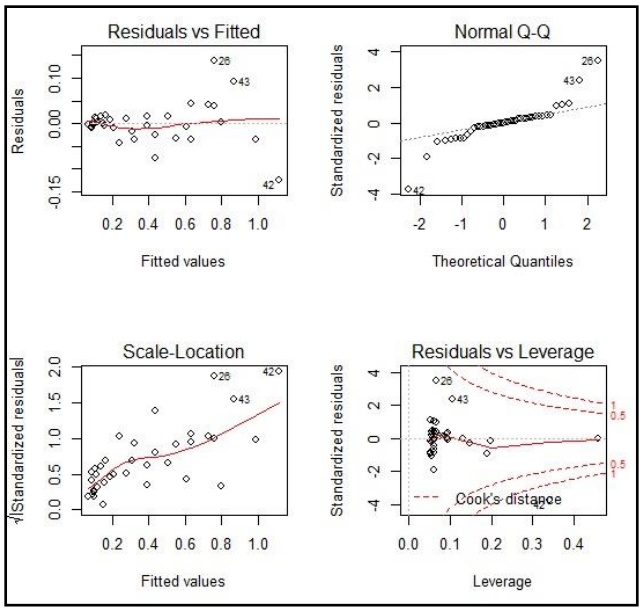

Figure 17. Data Testing Performance of Selected Model

The standard residual plot of Figure 17 showed the linearity and heteroscedasticity were good; the normal quantile plot showed the data were normally distributed; the scale-location plot showed the residual spreading equally along the ranges of predictors; and the Cook's distance line was close to a straight line without any leverage.

Therefore, our model for "Visibility" is:

$$\text{Risk} = \text{Vis}+\text{I(Vis\^{}2)}+\text{I(Vis\^{}3)}= 1.464-0.055\text{Vis}+ 7.49*10^{-4}\ \text{Vis}^2 -3.44*10^{-6}\ \text{Vis}^3 \quad (24)$$

Then the model was validated by applying K-fold cross validation (k=5), shown in Appendix 3 (Figure 6). Finally, the rest of the dataset were used to test the model. The mean value and standard deviation of the prediction were calculated to prove that the accuracy of our model was acceptable.

Therefore, by inputting the "Visibility" data into the model, the risk utility value for location A: Ua(V) = 0.5803 while the RUV for location B: Ub(V) = 0.3952. By the same process, the RUV of "windy days", Ua(W) = 0.2321 and Ub(W) = 0.1991; the RUV of "Following Current Probability", Ua(C) = 0.5218 and Ub(C) = 0.4281.

5.1.3 Weight Value Determination

The same methodology was applied to get the utility values of "windy days" and "following current Probability". Then the AHP was adopted to calculate weight values of each attribute. By applying pairwise comparison, the weight evaluation matrix of "Collision" can be obtained as shown in Table 15.

Table 15. Weight Evaluation Matrix of "Collision"

Evaluation Index	K_1	K_2	K_3
K_1, Visibility	**1**	**1.37**	**4.35**
K_2, Windy Days	**0.73**	**1**	**2.86**
K_3, Following Current Prob.	**0.23**	**0.35**	**1**

By calculation, the maximum eigenvalue of evaluation matrix is $\lambda_{max} = 3.0018$, and the weight vector (eigenvector) can be obtained accordingly. After normalizing, the weight vector is $W_A = (0.5146, 03628, 0.1226)$. Therefore, the consistency index is given as:

$$CI = \frac{\lambda_{\max} - n}{n-1} = \frac{3.0018-3}{3-1} = 0.0009 \tag{25}$$

To measure the scale of consistency index reasonably, the Saaty's average random consistency scale, RI, was introduced [7].

Five hundred comparison matrixes were randomly constructed, shown as $A_1, A_2, \cdots, A_{500}$, thus 500 eigenvaule can be calculated as $CI_1, CI_2, \cdots, CI_{500}$. The value of RI was calculated by the below formula.

$$RI = \frac{CI_1 + CI_2 + \cdots CI_{500}}{500} = \frac{\frac{\lambda_1 + \lambda_2 + \cdots + \lambda_{500}}{500} - n}{n-1} \tag{26}$$

The Saaty's average random consistency scale value [7], RI, is shown in Table 16.

Table 16. Average Random Consistency Scale Value by Saaty, 1990 [7]

n	1	2	3	4	5	6	7
RI	**0**	**0**	**0.58**	**0.90**	**1.12**	**1.24**	**1.32**

From the above table, the consistency rate is shown below.

$$CR = \frac{CI}{RI} = \frac{0.0009}{0.58} = 0.00155 < 0.1 \tag{27}$$

The output shows a satisfied consistency, thus the weight vector passed the consistency test. The weight vector for the attribute hierarchy of "Collision" is:

$$W_A = (K_1, K_2, K_3) = (0.5146, 03628, 0.1226) \tag{28}$$

Therefore, the RUV for "Collision",

$$\mathrm{Ua(Collision)} = \mathrm{k1} * \mathrm{Ua(V)} + \mathrm{k2} * \mathrm{Ua(W)} + \mathrm{k3} * \mathrm{Ua(C)} = 0.5146 * 0.5803 + 0.3628 * 0.2321 + 0.1226 * 0.5218 = 0.4468 \quad (29)$$

$$\mathrm{Ub(Collision)} = \mathrm{k1} * \mathrm{Ub(V)} + \mathrm{k2} * \mathrm{Ub(W)} + \mathrm{k3} * \mathrm{Ub(C)} = 0.5146 * 0.3952 + 0.3628 * 0.1991 + 0.1226 * 0.4281 = 0.3281 \quad (30)$$

$$\mathrm{Ua(Grouding)} = \mathrm{k1} * \mathrm{Ua(CW)} + \mathrm{k2} * \mathrm{Ua(CC)} + \mathrm{k3} * \mathrm{Ua(UKC)} = 0.4150 * 0.8513 + 0.2312 * 0.4417 + 0.3538 * 0.6616 = 0.6895 \quad (31)$$

$$\mathrm{Ub(Grouding)} = \mathrm{k1} * \mathrm{Ub(CW)} + \mathrm{k2} * \mathrm{Ub(CC)} + \mathrm{k3} * \mathrm{Ub(UKC)} = 0.4150 * 0.6731 + 0.2312 * 0.5709 + 0.3538 * 0.4013 = 0.5533 \quad (32)$$

According to previous incident records in Table 1, the ration of LNGC collision probability and LNGC grounding probability were 442/293. The weight value can be normalized as K(Collision) = 0.6013 and K(Grounding) = 0.3987.

The RUV of navigational process for location A is:

$$\mathrm{Ua(NP)} = \mathrm{k(Collision)} * \mathrm{Ua(Collision)} + \mathrm{k(Grounding)} * \mathrm{Ua(Grounding)} = 0.6013 * 0.4468 + 0.3987 * 0.6895 = 0.5436 \quad (33)$$

The RUV of navigational process for location B is:

$$\mathrm{Ub(NP)} = \mathrm{k(Collision)} * \mathrm{Ub(Collision)} + \mathrm{k(Grounding)} * \mathrm{Ub(Grounding)} = 0.6013 * 0.3281 + 0.3987 * 0.5533 = 0.4179 \quad (34)$$

For the berthing process, the weight value ratio of two identified hazards, "Contacting with the nearest obstruction", K(Obstruction) and the "Contacting with LNG FSRU", K(FSRU), was supposed as 7/13 due to the potential consequences. The

similar theory was applied to calculate the RUV of berthing process for two locations [40].

$$\mathrm{Ua(BP)} = \mathrm{k(Obstruction)} * \mathrm{Ua(Obstruction)} + \mathrm{k(FSRU)} * \mathrm{Ua(FSRU)} = 0.2680 * 0.3709 + 0.7380 * 0.4620 = 0.4404 \quad (35)$$

$$\mathrm{Ub(BP)} = \mathrm{k(Obstruction)} * \mathrm{Ub(Obstruction)} + \mathrm{k(FSRU)} * \mathrm{Ub(FSRU)} = 0.2680 * 0.3825 + 0.7380 * 0.5100 = 0.4789 \quad (36)$$

5.2 Evaluation Methodology for Chemical Process Safety Study

For LNG transferring process, the index of potential loss of life (PLL) was applied to evaluate the risk level of each alternative and the utility value can be determined by the potential facilities of MCS and WCS [41].

To obtain the PLL value of jet fire and pool fire, the thermal radiation distance [43], shown in Table 12, was employed to determine the possible fatality in the vulnerable areas.

Referred from Sudheer, S., et al., 2013 and Horn, et al., 2017, the consequences of thermal heat flux on human bodies were illustrated in Table 17.

Table 17. Thermal Radiation Intensity Impacts on Human Body (Adapted from [44] [45])

Heat Flux (kW/m^2)	Impacts on one human body
1.4	Harmless for human body
2.1	Minimum required to cause pain after 1 minute
4.0	Pain after 20-second exposure, cause first degree burns
7.0	Maximum tolerable for firefighters with completed covered protective clothes
12.5	Extreme pain within 20-second exposure; Lethality if escape not possible
25.0	Mechanical integrity of insulated thin steel can be lost
37.5	Collapse of mechanical structures; Instantaneous lethality

To establish the relationship between fatality and thermal radiation intensity, the theory of probit functions should be presented. A Thermal Dose Unit (TDU) defined in equation 5 is a unit to measure exposure to thermal radiation [52].

$$V = I^{4/3}t \tag{37}$$

Where

-I: the intensity of thermal radiation

-t: the exposure time

Then the equation 6 was built to establish relationship between probit function Y and the thermal dose V.

$$Y = a + bInV \tag{38}$$

Where

-a, -b: the coefficients of probit function

-V: the thermal dose

Typically, the probit function for was firstly proposed by Eisenberg in 1975 based on nuclear explosion data [46]. Then Tsao and Perry modified Eisenberg's model by considering infrared radiation and Lees presented his model by validating on pig skin experiments [47]. By taking into account the protection effects of clothes, TNO Green Book showed an advanced model to be widely applied to determine the lethality.

Table 18. Summary of Probit Function Models

Model	a	b	Key Publications
Eisenberg's Model	-14.9	2.56	[46], [50]
Tsao & Perry's Model	-12.8	2.56	[47], [51]
Lees's Model	-10.69	1.99	[48], [51]
TNO Model	-13.65	2.56	[49], [51]

The vulnerable building for two alternatives should be determined to calculate PPL value. Three ranges (500-meter circle, 1000-meter circle and 1500-meter circle) were drawn in Figure 18 to show potential damaged buildings for location A.

Figure 18. Vulnerable Areas for Location A under 500m Circle, 1000m Circle and 1500m Circle

For location A: In the range of 500-meter radius area (the left side figure in Figure 20), there are one working station and three LNG tanks; the number of workers in this area is assumed as 69. In the range of 1000-meter radius area (the middle one in Fig. 20), there are one residential area with 500 people, one berth for importing ore, one office building for ore company and two more working stations, assuming the total number of people involved is 694. In the range of 1500 meters, there are one police station, four more working stations, one more ore-ship berth, 3 storage warehouses and 15 storage tanks and one more grocery retailer shop; the maximum number of involved people for WCS in this area is assumed as 849, and the number of involved personnel for MCS was assumed as 70% of the maximum number.

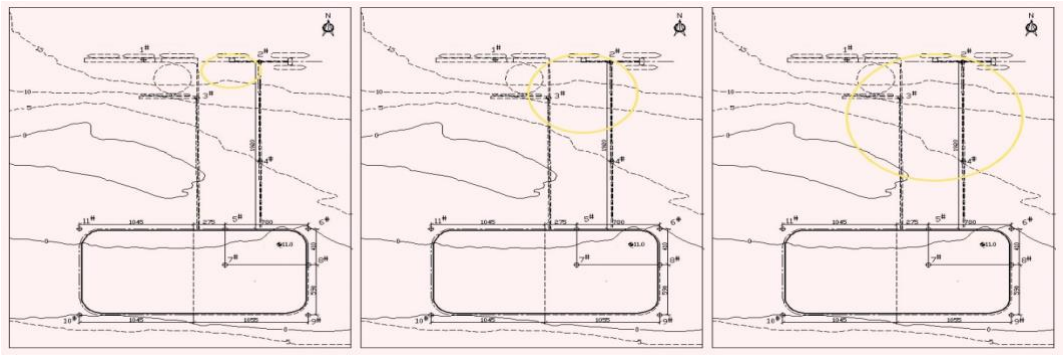

Figure 19. Vulnerable Areas for Location B under 500m Circle, 1000m Circle and 1500m Circle

Figure 19 shows the vulnerable areas (marked with yellow circles) with the radius of 500 meters (left side figure), 1000 meters (middle one) and 1500 meters (right side figure) for location B. The coast line of Qidong port area was surrounded by shallow shoals. Therefore, two pipeline bridges were built to extend 1.5 km to the sea to allow large-scale ships to safely get alongside Qidong port. As a result of the two bridges, less vulnerable buildings were involved in the influential areas. For 500-meter radius area, the only influential building is one pipeline bridge except the LNG FSRU system; for 1000-meter radius area, there are one turning basin, one bulk-carrier berth and two pipeline bridges; besides that, there is one more crude oil berth in the 1500-meter radius of proposed LNG FSRU system. Suppose three people working for every 500 meters on the pipeline bridges, four tug boats with total 52 workers on board in turning basin, 30 people in LNG carrier and crude oil tanker and 25 in bulk carrier, and 10 people for loading/unloading operations for each vessel. So, the maximum numbers of people involved for WCS in the three vulnerable areas were estimated as 38, 124 and

164, respectively; also, the number of involved personnel for MCS was assumed as 70% of the maximum values.

On the other hand, the PLL of flash fire was calculated by the values of LFL and 0.5 LFL. The possibility of fatality was assumed 100% in Zone 1, a defined zone between UFL contour and LFL contour; and 50% for Zone 2, defined between LFL contour and 0.5LFL contour [46].

Referred by DNVGL MPACT Model [53], the heat flux value "4kW/m^2" could lead to 1% possible fatality, while the value of "12.5 kW/m^2" was 50% and the value of "37.5 kW/m^2" was 100%. As for the range between these three point values, the lethality ellipse, see Figure 19, was employed to calculate the PLL in this study.

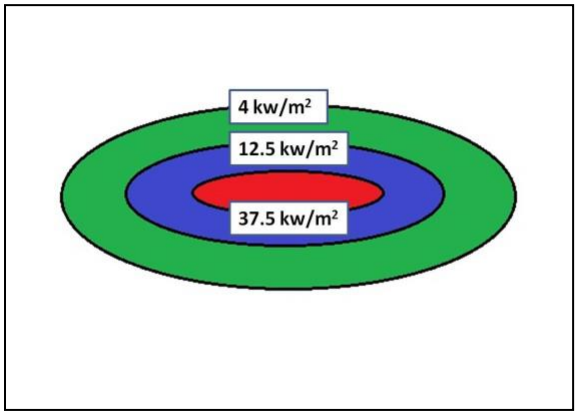

Figure 20. Defined Heat Flux Impact Area

From the above figure, three point values were shown as the barrier value of three areas. The Red Zone, which was defined as the most vulnerable area with the heat flux value larger than 37.5 km/m2, while the Blue Zone was the area with that value

between 12.5 and 37.5; the Green Zone was the area with the heat flux value between 4 and 12.5. The average possibility of fatality (APF) was set as 1.0 in the red area, while the APF of blue area was 0.75 and that of the green area was 0.255 [53].

According to the Table 10, the PLLs of location A and location B under MCS and WCS were calculated shown in below table.

Table 19. Summary of PLL for Simulation Runs

Plan	Loc.	Scenario	Fire Type	Involved Vulnerable Buildings	Potential Involved Personnel	PLL	Thermal Radiation Distance			Flammability Limits Distance		
							4kW/m^2	12.5kW/m^2	37.5kW/m^2	UFL	LFL	0.5LFL
1	A	MCS	Flash	Working stations (7), LNG tanks (3), residential area (1), LNG FSRU system (1), berth (2), office building (1), warehouses (3), storage tanks (15), grocery shop (1), police station (1)	Zone 1:301; Zone 2: 76	339				220	794	1590
2	A	WCS	Jet	Working stations (3), LNG tanks (3), residential area (1), berth (1), LNG FSRU system (1), office building (1)	Red Zone: 694; Blue Zone: 10; Green Zone: 15	706	1141	1022	976			
3	B	MCS	Flash	LNG FSRU system (1), berth (2), pipeline bridge (2), turning basin (1)	Zone 1:78; Zone 2: 38	97				194	771	1546
4	B	WCS	Jet	LNG FSRU system (1), berth (1), pipeline bridge (2), turning basin (1)	Red Zone: 124; Blue Zone: 15; Green Zone: 25	142	1128	1016	976			
5	A	MCS	Flash	Working stations (1), LNG tanks (1), LNG FSRU system (1)	Zone 1:14; Zone 2: 28	28				11	77	277
6	A	WCS	Pool	Working stations (1), LNG tanks (3), LNG FSRU system (1)	Red Zone: 40; Blue Zone: 20; Green Zone: 9	58	501	302	192			
7	B	MCS	Flash	LNG FSRU system (1), pipeline bridge (1)	Zone 1:14; Zone 2: 10	19				9	70	202
8	B	WCS	Pool	LNG FSRU system (1), berth (1), pipeline bridge (2), turning basin (1)	Red Zone: 32; Blue Zone: 17; Green Zone: 35	54	722	525	222			

The probability 10^{-5} per year was usually defined as the boundary of the individual risk of fatality for marine transfer operation [50]. This frequency was assumed as the total frequency of Event A "connection flange failure" and Event B "connection hose failure", and the Pr(A) was assumed as $2.5 * 10^{-6}$, then Pr(B) equals to $7.5*10^{-6}$.

The frequency of each scenario can be obtained from the event tree analysis (see Appendix 4), so the value of risk can be calculated by PLL timing frequency.

Under the Maximum Credible Scenario,

$$R_a(MCS) = R_a(\text{Event A}) + R_a(\text{Event B}) = 1.047*10^{-4} \text{ deaths per year} \quad (39)$$

$$R_b(MCS) = R_b(\text{Event A}) + R_b(\text{Event B}) = 3.811*10^{-5} \text{ deaths per year} \quad (40)$$

For Worst Case Scenario,

$$R_a(WCS) = R_a(\text{Event A}) + R_a(\text{Event B}) = 1.809*10^{-4} \text{ deaths per year} \quad (41)$$

$$R_b(WCS) = R_b(\text{Event A}) + R_b(\text{Event B}) = 3.955*10^{-5} \text{ deaths per year} \quad (42)$$

Based on the ALARP boundaries defined by International Maritime Organization (IMO), the risk utility scale was built accordingly, see Table 20.

Table 20. Evaluation Scale for "PLL per Year"

Utility / Range / Factors	Favorable, (0.8,1]	Acceptable, (0.6,0.8)	Moderate, (0.4,0.6]	Limited Acceptable, (0.2,0.4]	Unacceptable, [0,0.2]
PLL per year	$<10^{-6}$	10^{-5}~10^{-6}	10^{-4}~10^{-5}	10^{-3}~10^{-4}	$>10^{-3}$

Therefore, the risk value was converted to utility value on the basis of linear relation between utility range and PLL value. For MCS, the weight values of "Event A" and "Event B" were 0.25, 0.75, respectively. For "WCS", the weight values of "Event A" and "Event B" were 0.75 and 0.25. Then the utility values for location A and location B under MCS condition are:

$$Ua(MCS)= k_1U(Event\ A)+k_2U(Event\ B) = 0.25*0.4358+0.75*0.5760 = 0.5410 \quad (43)$$

$$Ub(MCS)= k_1U(Event\ A)+k_2U(Event\ B) = 0.25*0.5689+0.75*0.5909 = 0.5854 \quad (44)$$

For WCS, the utility values of two locations are:

$$Ua(WCS) = k_1U(Event\ A)+k_2U(Event\ B) = 0.75*0.3830 + 0.25*0.7256 = 0.4687 \quad (45)$$

$$Ub(WCS) = k_1U(Event\ A)+k_2U(Event\ B) = 0.75*0.5433+0.25*0.7322 = 0.5905 \quad (46)$$

5.3 Total Utility Value Calculation

From Table 1, the probabilities of collision, grounding, contact, fire & explosion and loading/unloading events were converted to the ratio to calculate the weight value of navigational process, berthing process and LNG transferring process. Therefore, k(NP) = 0.7541; k(BP) = 0.1498; k(TP) = 0.0961.

The total utility value for location A under MCS is:

$$U_a = k_1U_a(NP) + k_2U_a(BP) + k_3U_a(TP) = 0.5225 \quad (47)$$

The total utility value for location A under MCS is:

$$U_b = k_1U_b(NP) + k_2U_b(BP) + k_3U_b(TP) = 0.4431 \quad (48)$$

Under WCS, U_a'= 0.5212; U_b'= 0.4436.

CHAPTER VI

CONCLUSIONS AND RECOMMENDATIONS

In summary, the total utility value showed location A was a more reliable place to build the LNG FSRU system. Generally, the two values both located in the utility range (0.4, 0.6), reckoned as "Moderate". Specifically, some further conclusions can be achieved by different processes.

For navigational process, location A outperformed location on both "collision" and "grounding", proving the navigation environment of location A was more reliable for LNG carriers than that of location B; for berthing process, location B had a higher overall score, showing it was less risky for identified contacting with berthing obstructions and LNG FSRU. For LNG transferring process, two events and two scenarios were identified for LNG accidental release, location B performed better than location A on both of two events as it separated the populated areas with two pipeline bridges so that less vulnerable buildings were involved in the vicinity of location B. Although location B outperformed location A in two of three processes, location A still had a higher score in the total utility value since the weight value for navigational process was much larger than other two processes based on the recorded incidents.

To mitigate the risk into an acceptable level, some measures may be taken into account. For navigational process, the security zones, both static and dynamic zones, should be set up for large scale LNG carriers, such as Q-Flex and Q-Max, to avoid other

traffic interfering LNGC, and this measure can reduce the occurrence of collision in inbound channels significantly [38, 54]; the recommended routes should be always top priority to navigate since the UKC can meet the requirement of safe sailing or large draft vessels may ride on the tide to pass the shallow areas. For berthing process, enough turning basin, especially enough berthing width should be ensured to lower the risk of contact with FSRU or other navigational hazards, and the transverse speed of the LNGC should be observed frequently when it is approaching the LNG FSRU. For LNG transferring process, the emergency plan and procedures should be implemented before the operation begins; the responsible officers should be assigned to ensure every possible contingency could follow an organized procedure; evacuation plans and extreme situation trainings were the key factors to succeed in potential disasters.

This research serves as a quantitative way to evaluate the three consecutive processes for one engineering system, LNG FSRU system. It is a trail to apply both nautical study and chemical process safety knowledge on near shore industry. In the evaluation process, the objective environmental factors were deeply compared via simulation and statistical software. However, human factors and other subjective uncertainties are necessary to consider under different hydrographic and meteorological conditions for the LNG FSRU system. From the perspective of offshore safety, this data-driven direction would be a right way to make safety the second nature. To accomplish this goal step by step, more data sources should be added to monitor operations in different dimensions and more data analytic methodologies should be applied to build a clearer relationship between raw data and safety performances.

REFERENCES

[1] Zednik, Jay J., David L. Dunlavy, and Thomas G. Scott. "Regasification of liquefied natural gas (LNG) aboard a transport vessel." U.S. Patent No. 6,089,022. 18 Jul. 2000.

[2] Andersson, Henrik, Marielle Christiansen, and Kjetil Fagerholt. "Transportation planning and inventory management in the LNG supply chain." Energy, natural resources and environmental economics. Springer Berlin Heidelberg, 2010. 427-439.

[3] Aronsson, E.R.I.K. "FLNG compared to LNG carriers." Requirements and recommendations for LNG production facilities and re-gas units. Chalmers University of Technology, Gothenburg Sweden (2012).

[4] Tatiana Morosuk and George Tsatsaronis (2012). LNG – Based Cogeneration Systems: Evaluation Using Exergy-Based Analyses, Natural Gas - Extraction to End Use, Dr. Sreenath Gupta (Ed.), InTech, DOI: 10.5772/51477. Available from: https://www.intechopen.com/books/natural-gas-extraction-to-end-use/lng-based-cogeneration-systems-evaluation-using-exergy-based-analyses

[5] Finn, Adrian J. "Effective LNG production offshore." 81 st Annual GPA Convention. 2002.

[6] Shapira, Aviad, and Marat Goldenberg. "AHP-based equipment selection model for construction projects." Journal of Construction Engineering and Management 131.12 (2005): 1263-1273.

[7] Thomas L. Saaty. How to make a decision: The Analytic Hierarchy Process [J]. European Journal of Operational Research, 48 (1990): 9-26.

[8] Paltrinieri, Nicola, Alessandro Tugnoli, and Valerio Cozzani. "Hazard identification for innovative LNG regasification technologies." Reliability Engineering & System Safety 137 (2015): 18-28.

[9] Woodward, John L., and Robin Pitbaldo. LNG Risk Based Safety: modeling and consequence analysis. John Wiley & Sons, 2010.

[10] Fujii, Teruo, et al. "Multilayered reinforcement learning for complicated collision avoidance problems." Robotics and Automation, 1998. Proceedings. 1998 IEEE International Conference on. Vol. 3. IEEE, 1998.

[11] Macduff, T. "The probability of vessel collisions." Ocean Industry 9.9 (1974).
[12] Pedersen, P. Terndrup, and Shengming Zhang. "On impact mechanics in ship collisions." Marine Structures 11.10 (1998): 429-449.

[13] Li, Suyi, Qiang Meng, and Xiaobo Qu. "An overview of maritime waterway quantitative risk assessment models." Risk Analysis 32.3 (2012): 496-512.

[14] Pedersen, S., V. Simonsen, and V. Loeschcke. "Overlap of gametophytic and sporophytic gene expression in barley." TAG Theoretical and Applied Genetics 75.1 (1987): 200-206.

[15] Montewka, J., et al. "Marine traffic risk modelling–an innovative approach and a case study." Proceedings of the Institution of Mechanical Engineers, Part O: Journal of Risk and Reliability 225.3 (2011): 307-322.

[16] Yansheng, Yang. "Study on mathematical model for simulating ship berthing or unberthing [J]." Journal of Dalian Maritime University 4 (1996).

[17] Lei Fu. Safety Assessment and Research on Liquified Carriers in Huangdao of Qingdao Port Area, MS thesis. Dalian Maritime University, 2014

[18] Jun Bai. Simulation of Large Vessel Berthing Maneuvering MS thesis. Dalian Maritime University, 2010

[19] Winbow, A. "The importance of effective communication." International Seminar on Maritime English. 2002.

[20] Xiu-Feng, Zhang, Yin Yong, and Jin Yi-Cheng. "Ship motion mathematical model with six degrees of freedom in regular wave [J]." Journal of Traffic and Transportation Engineering 3 (2007): 008.

[21] Liu, Y., et al. "Numerical studies of two side-by-side elastic cylinders in a cross-flow." Journal of Fluids and Structures 15.7 (2001): 1009-1030.

[22] Ventikos, Nikolaos P., and Dimitrios I. Stavrou. "Ship to Ship (STS) Transfer of Cargo: Latest Developments and Operational Risk Assessment." SPOUDAI-Journal of Economics and Business 63.3-4 (2013): 172-180.

[23] Abbasi, Tasneem, H. J. Pasman, and Sakineh A. Abbasi. "A scheme for the classification of explosions in the chemical process industry." Journal of hazardous materials 174.1 (2010): 270-280.

[24] Luketa-Hanlin, Anay. "A review of large-scale LNG spills: experiments and modeling." Journal of hazardous materials 132.2 (2006): 119-140.

[25] Fay, J. A. "Spread of large LNG pools on the sea." Journal of Hazardous Materials 140.3 (2007): 541-551.

[26] Hightower, Mike, et al. Guidance on risk analysis and safety implications of a large liquefied natural gas (LNG) spill over water. Sandia National Labs Albuquerque NM, 2004.

[27] Bowen, Ronald Ray, et al. "LNG Technology Advances and Challenges." International Petroleum Technology Conference. International Petroleum Technology Conference, 2008.

[28] Regualtions for Use of the Liquefied Natural Gas Terminal SC Klaipedos Nafta, 2016.

[29] Chenxi Ji, Shicai Chen and Haibo Xie. Research on Feasible Degree of Navigation Environment for CALM Type Single Point Mooring System. Journal of Dalian Maritime University, 2014(2). 29-32.

[30] Code for Design of Liquefied Natural Gas Port and Jetty (JTS 165-5-2016).

[31] Raj, Phani K., and Leon A. Bowdoin. "Underwater LNG release: Does a pool form on the water surface? What are the characteristics of the vapor released?." Journal of Loss Prevention in the Process Industries 23.6 (2010): 753-761.

[32] D'alessandro, A. A., E. M. Izurieta, and S. M. Tonelli. "Decision-making tools for a LNG regasification plant siting." Journal of Loss Prevention in the Process Industries 43 (2016): 255-262.

[33] Pitblado R, Baik J, Raghunathan V. LNG decision making approaches compared[J]. Journal of hazardous materials, 2006, 130(1): 148-154.

[34] Kim, K., K. Park, M.S. Mannan and E.S. Yoon, "Safety Analysis of LNG Terminal Focused on the Consequence Calculation of Accidental and Intentional Spills," Proceedings of the 8th Annual Mary Kay O'Connor Process Safety Center Symposium – Beyond Regulatory Compliance: Making Safety Second Nature, College Station, Texas, October 25-26, 2005, pp. 200-218.

[35] Spouge, J., 1999. A guide to quantitative risk assessment for offshore installations The centre for Marine and Petroleum Technology (CMPT).

[36] Freeman, R. A. (1990). CCPS guidelines for chemical process quantitative risk analysis. Plant/Operations Progress, 9(4), 231-235.

[37] ZHANG, Bin, Wan-qing WU, and Gui-feng YU. "Risk and hazard analysis for LNG spillage over water [J]." Journal of Dalian Maritime University 4 (2006): 020.

[38] Ma, Hui and Zhaolin Wu. "Evaluation and analysis on danger degree of port shipoperating environment by Grey System Theory [J]." JOURNAL OF DALIAN MARITIME UNIVERSITY 3 (1998).

[39] Vanem, Erik, et al. "Analysing the risk of LNG carrier operations." Reliability Engineering & System Safety 93.9 (2008): 1328-1344.

[40] Hsu, Wen-Kai Kevin. "Assessing the Safety Factors of Ship Berthing Operations." Journal of Navigation 68.03 (2015): 576-588.

[41] Raj, Phani K. "Large LNG fire thermal radiation—modeling issues and hazard criteria revisited." Process Safety Progress 24.3 (2005): 192-202.

[42] Witlox, H., M. Harperm, and Robin Pitblado. "Validation of PHAST dispersion model as required for USA LNG siting applications." Chemical Engineering Transactions 31 (2013).

[43] Pitblado, R. M., et al. "Consequences of liquefied natural gas marine incidents." Process safety progress 24.2 (2005): 108-114.

[44] Sudheer, S., et al. "Fire safety distances for open pool fires." Infrared Physics & Technology 61 (2013): 265-273.

[45] Horn, Matthew, Dagmar Schmidt Etkin, and Andrew Wolford. "Quantitative evaluation of risks from crude-by-rail spills: A case study using the proposed Shell Puget Sound Refinery Anacortes Rail Unloading Facility." International Oil Spill Conference Proceedings. Vol. 2017. No. 1. International Oil Spill Conference, 2017.

[46] Eisenberg, Norman A., Cornelius J. Lynch, and Roger J. Breeding. Vulnerability model. A simulation system for assessing damage resulting from marine spills. Enviro control inc rockville md, 1975.

[47] Tsao, Chi K., and Willard W. Perry. Modifications to the vulnerability model: a simulation system for assessing damage resulting from marine spills. Enviro Control INC Rockville MD, 1979.

[48] Lees, Frank P. "The assessment of major hazard: a model for fatal injury from burns." Process safety and environmental protection72.3 (1994): 127-134.

[49] TNO Green Book. "Methods for the determination of possible damage to people and objects resulting from releases of hazardous materials." Report CPR E 16 (1992).

[50] Marin, "Nautical And Risk Studies for the Delimara LNG Terminal in Marsaxlokk Port, Malta. Item 6: Nautical Quantitative Risk Assessment (QRA) Report," 2016.

[51] Sam Mannan, ed. Lees' loss prevention in the process industries. Butterworth-Heinemann, 2005: 1306-1310.

[52] O'Sullivan, S., and S. Jagger. Human vulnerability to thermal radiation offshore. Health & Safety Laboratory, 2004.

[53] DNVGL, Theory MPACT Mode, 2016.

[54] M.F. Pantony, Hazards XVII: Process Safety : Fulfilling Our Responsibilities (2003): 666-667.

[55] DNVGL, Theory Jet Fire, 2016.

[56] DNVGL, Theory Pool Fire Model, 2016.

[57] Dalian Maritime University, Formal Safety Assessment Report of Dalian LNG Terminal Project, 2011: 11-13.

APPENDIX 1

Sample Questionnaire for Risk Utility Value of LNG FSRU Evaluation Attributes

Which department are you in?

1. Maritime Institutes
2. Pilot Station
3. Shipping Companies

How many years have you worked/researched for LNG carriers?

1. Less than 5years
2. 5 to 8 years
3. More than 8 years

The evaluation scale was set between 0 and 1, and five evaluation ranges were determined with the even interval of 0.2 based on the risk level for LNG FSRU system, see table below.

Table. 1-1 Quantitative Value for Risk Qualitative Evaluation

Favorable	Acceptable	Moderate	Limited Acceptable	Unacceptable
[0.8,1]	[0.6,0.8)	[0.4,0.6)	[0.2,0.4)	[0,0.2)

Risk utility value range from 0.8 to 1.0 means the environment of this location is favorable to build LNG FSRU, while the value locating between 0.6 and 0.8 means it is acceptable for LNG FSRU; the range 0.4 to 0.6 means moderate environmental conditions for the system; limited acceptable when the risk utility value is in the range of 0.2 to 0.4.

Risk Evaluation for "Visibility"

Visibility value for LNG carrier is defined as the number of days under poor visibility (visible distance < 4000m) per year. Now please fill the blanks about the relevant values.

Which value do you think is the most appropriate one when risk utility value of "Visibility" is set as 0.2, 0.4, 0.6 and 0.8, respectively? Please fill the blanks.

Table. 1-2 "Visibility" Evaluation Table

	Risk Utility Value= 0.2	Risk Utility Value= 0.4	Risk Utility Value= 0.6	Risk Utility Value= 0.8
Restricted Visibility Days per Year				

APPENDIX 2

```
> boxplot(data1)
> data1=read.table("clipboard",header=T)
> boxplot(data1)
> t.test(data1)

        One Sample t-test

data:  data1
t = 51.332, df = 87, p-value < 2.2e-16
alternative hypothesis: true mean is not equal to 0
95 percent confidence interval:
 14.47380 15.63983
sample estimates:
mean of x
 15.05682

> boxplot(data1)
> t.test(data1)

        One Sample t-test

data:  data1
t = 110.16, df = 84, p-value < 2.2e-16
alternative hypothesis: true mean is not equal to 0
95 percent confidence interval:
 29.1465 30.2182
sample estimates:
mean of x
 29.68235
```

```
> data1=read.table("clipboard",header=T)
> boxplot(data1)
> t.test(data1)

        One Sample t-test

data:  data1
t = 78.801, df = 82, p-value < 2.2e-16
alternative hypothesis: true mean is not equal to 0
95 percent confidence interval:
 19.68300 20.70254
sample estimates:
mean of x
 20.19277

> data1=read.table("clipboard",header=T)
> boxplot(data1)
> t.test(data1)

        One Sample t-test

data:  data1
t = 181.11, df = 80, p-value < 2.2e-16
alternative hypothesis: true mean is not equal to (
95 percent confidence interval:
 39.76803 40.65172
sample estimates:
mean of x
 40.20988
```

Figure 2-1. Outputs of Confidential Interval of "Visibility" Threshold

APPENDIX 3

```
> lm.fit=lm(Risk~Vis, data=data1)
> summary(lm.fit)

Call:
lm(formula = Risk ~ Vis, data = data1)

Residuals:
     Min       1Q   Median       3Q      Max
-0.19608 -0.12252 -0.01319  0.12838  0.27082

Coefficients:
             Estimate Std. Error t value Pr(>|t|)
(Intercept)  0.8303064  0.0440807   18.84   <2e-16 ***
Vis         -0.0108557  0.0009122  -11.90    7e-15 ***
---
Signif. codes:  0 '***' 0.001 '**' 0.01 '*' 0.05 '.' 0.1 ' ' 1

Residual standard error: 0.1407 on 41 degrees of freedom
Multiple R-squared:  0.7755,    Adjusted R-squared:   0.77
F-statistic: 141.6 on 1 and 41 DF,  p-value: 7.005e-15
```

Figure 3-1. For "Risk= $\beta_0+\beta_1$Vis"

```
> lm.fit=lm(Risk~log(Vis), data=data1)
> summary(lm.fit)

Call:
lm(formula = Risk ~ log(Vis), data = data1)

Residuals:
      Min        1Q    Median        3Q       Max
-0.115569 -0.060755 -0.001431  0.057830  0.183096

Coefficients:
             Estimate Std. Error t value Pr(>|t|)
(Intercept)  1.93130    0.06452   29.93   <2e-16 ***
log(Vis)    -0.43800    0.01784  -24.56   <2e-16 ***
---
Signif. codes:  0 '***' 0.001 '**' 0.01 '*' 0.05 '.' 0.1 ' ' 1

Residual standard error: 0.07494 on 41 degrees of freedom
Multiple R-squared:  0.9363,    Adjusted R-squared:  0.9348
F-statistic:   603 on 1 and 41 DF,  p-value: < 2.2e-16
```

Figure 3-2. For "Risk= $\beta_0+\beta_1$In(Vis)"

```
> summary(lm.fit)

Call:
lm(formula = Risk ~ Vis + I(Vis^2), data = data1)

Residuals:
      Min        1Q    Median        3Q       Max
-0.112369 -0.036073  0.004677  0.040416  0.143156

Coefficients:
             Estimate Std. Error t value Pr(>|t|)
(Intercept)  1.251e+00  3.279e-02   38.14   <2e-16 ***
Vis         -3.495e-02  1.637e-03  -21.35   <2e-16 ***
I(Vis^2)     2.555e-04  1.694e-05   15.08   <2e-16 ***
---
Signif. codes:  0 '***' 0.001 '**' 0.01 '*' 0.05 '.' 0.1 ' ' 1

Residual standard error: 0.05511 on 40 degrees of freedom
Multiple R-squared:  0.9664,    Adjusted R-squared:  0.9647
F-statistic: 575.5 on 2 and 40 DF,  p-value: < 2.2e-16
```

Figure 3-3. For "Risk= $\beta_0+\beta_1$Vis+ β_2Vis^2"

```
> lm.fit=lm(Risk~Vis+I(Vis^2)+I(Vis^3), data=data1)
> summary(lm.fit)

Call:
lm(formula = Risk ~ Vis + I(Vis^2) + I(Vis^3), data = data1)

Residuals:
      Min        1Q    Median        3Q       Max
-0.124696 -0.009811  0.000220  0.012575  0.138456

Coefficients:
             Estimate Std. Error t value Pr(>|t|)
(Intercept)  1.464e+00  4.408e-02  33.224  < 2e-16 ***
Vis         -5.504e-02  3.662e-03 -15.030  < 2e-16 ***
I(Vis^2)     7.492e-04  8.583e-05   8.729 1.04e-10 ***
I(Vis^3)    -3.441e-06  5.918e-07  -5.814 9.38e-07 ***
---
Signif. codes:  0 '***' 0.001 '**' 0.01 '*' 0.05 '.' 0.1 ' ' 1

Residual standard error: 0.04085 on 39 degrees of freedom
Multiple R-squared:  0.982,     Adjusted R-squared:  0.9806
F-statistic: 709.6 on 3 and 39 DF,  p-value: < 2.2e-16
```

Figure 3-4. For "Risk= $\beta_0+\beta_1$Vis+ β_2Vis^2 +β_3Vis^3"

```
> lm.fit=lm(Risk~Vis+I(Vis^2)+I(Vis^3)+I(Vis^4), data=data1)
> plot(lm.fit)
> summary(lm.fit)

Call:
lm(formula = Risk ~ Vis + I(Vis^2) + I(Vis^3) + I(Vis^4), data = data1)

Residuals:
      Min        1Q    Median        3Q       Max
-0.093642 -0.016540 -0.000006  0.018339  0.132348

Coefficients:
             Estimate Std. Error t value Pr(>|t|)
(Intercept)  1.362e+00  7.141e-02  19.071  < 2e-16 ***
Vis         -4.131e-02  8.437e-03  -4.897 1.83e-05 ***
I(Vis^2)     1.870e-04  3.243e-04   0.577   0.5676
I(Vis^3)     5.337e-06  4.927e-06   1.083   0.2855
I(Vis^4)    -4.588e-08  2.557e-08  -1.794   0.0808 .
---
Signif. codes:  0 '***' 0.001 '**' 0.01 '*' 0.05 '.' 0.1 ' ' 1

Residual standard error: 0.03973 on 38 degrees of freedom
Multiple R-squared:  0.9834,    Adjusted R-squared:  0.9817
F-statistic: 563.2 on 4 and 38 DF,  p-value: < 2.2e-16
```

Figure 3-5. Risk= $\beta_0+\beta_1$Vis+ β_2Vis^2+β_3Vis^3 +β_4Vis^4

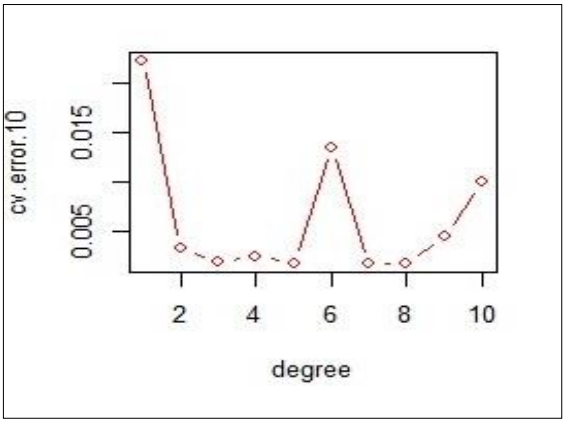

Figure 3-6. K-fold Cross Validation

APPENDIX 4

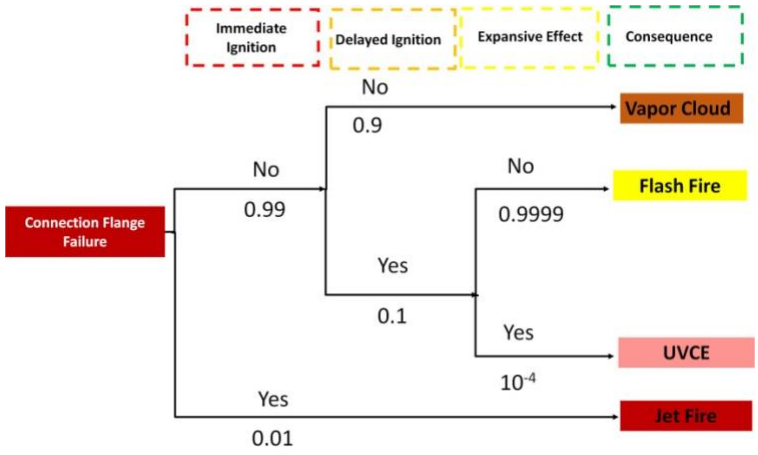

Figure 4-1. Event Tree for Connection Flange Failure

Note: UVCE stands for Unconfined Vapor Cloud Explosion, which was neglected in this research due to its tiny possibility.

Plan 1, Ra(Flash Fire) = Pr_1*PLL = $2.475*10^{-7}*339 = 0.839*10^{-4}$ deaths per year
Plan 2, Ra(Jet Fire) = Pr_2*PLL = $2.5*10^{-8}*706 = 1.765*10^{-4}$ deaths per year
Plan 3, Rb(Flash Fire) = Pr_3*PLL = $2.475*10^{-7}*97 = 0.240*10^{-4}$ deaths per year
Plan 4, Rb(Jet Fire) = Pr_4*PLL = $2.5*10^{-8}*142 = 0.355*10^{-4}$ deaths per year

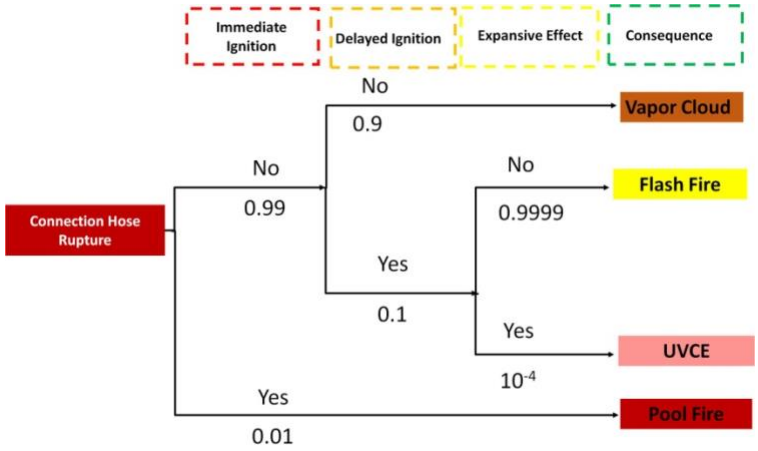

Figure 4-2. Event Tree for Connection Hose Rupture

Plan 5, Ra(Flash Fire) = Pr_5*PLL = $7.424*10^{-7}*28 = 2.079*10^{-5}$ deaths per year
Plan 6, Ra(Jet Fire) = Pr_6*PLL = $7.5*10^{-8}*58 = 0.435*10^{-5}$ deaths per year
Plan 7, Rb(Flash Fire) = Pr_7*PLL = $7.424*10^{-7}*19 = 1.411*10^{-5}$ deaths per year
Plan 8, Rb(Jet Fire) = Pr_8*PLL = $7.5*10^{-8}*54 = 0.405*10^{-5}$ deaths per year